FANCC REGULATES THE SPINDLE ASSEMBLY CHECKPOINT TO PREVENT TUMORIGENESIS IN VIVO

Donna Marie Edwards

Submitted to the faculty of the University Graduate School
in partial fulfillment of the requirements
for the degree
Doctor of Philosophy
in the Department of Biochemistry and Molecular Biology,
Indiana University

June 2017

Accepted by the Graduate Faculty of Indiana University, in partial fulfillment of the requirements for the degree of Doctor of Philosophy.

Doctoral Committee

_____
D. Wade Clapp, M.D., Chair

_____
Grzegorz Nalepa, M.D., Ph.D.

_____
Maureen A. Harrington, Ph.D.

March 27, 2017

_____
Mark G. Goebl, Ph.D.

ACKNOWLEDGEMENTS

To begin I offer my sincere gratitude to my two outstanding thesis mentors, Dr. Grzegorz Nalepa and Dr. Wade Clapp. They have been excellent role models for me—their enthusiasm for science is contagious, and both have done research that has directly improved patient care. I would like to thank them both for believing in me, challenging me scientifically to take risks and teaching me to communicate my findings in presentation and writing. They have been an inspiration to me, and I hope to one day have the opportunity to mentor the next generation of young scientists, as they have done for me.

I am also very thankful to my committee members Dr. Maureen Harrington and Dr. Mark Goebl for their thoughtful input on my work. I always enjoyed our scientific conversations, which left me with many new ideas and a renewed excitement to move the project forward.

I thank all the members of the Clapp and Nalepa laboratories who have helped me over the past four years. In particular, I would like to acknowledge Dr. Zejin Sun, Dr. Sierra Potchanant, Dr. Su-Jung Park, and Ying He for their guidance in teaching me experimental technique and design in the lab. I also appreciate the support and friendship of my fellow graduate student, Zahi Abdul Sater, who has taught me how to make beautiful scientific figures, and whose work greatly enhanced my thesis project.

I am grateful for the support and mentorship of the Medical Scientist Training Program, and many MSTP students for their special contributions. Karl Staser mentored me in my first laboratory experience as an undergraduate, and his enthusiasm for science was contagious--after that summer I knew I wanted to become a physician-scientist. Jeff Gehlhausen shared his creative ideas in many scientific brainstorming sessions with me, and I often turned to him for advice in the lab. I am also thankful to Stefan Tarnawsky, for always willing to lend a helping hand with flow cytometry and for his friendship throughout graduate school. I also would like to point out my MSTP classmates—Daniel Sassoon, Abass Conteh, Sherri Huang, Deborah Olmstead, Nick Race, Stefan Tarnawsky, and James Wodicka—I cannot thank them enough for their friendship and support throughout this program.

I would also like to thank my funding sources, which have included the Indiana Clinical and Translational Sciences Institute, and the National Cancer Institute.

Finally, I would whole-heartedly like to thank my husband, Daniel, and my parents, Bob and Sue, and brothers, Brian and Greg, for their love and encouragement in pursuing my dreams.

Donna Marie Edwards

FANCC REGULATES THE SPINDLE ASSEMBLY CHECKPOINT TO PREVENT TUMORIGENESIS IN VIVO

The Fanconi anemia (FA) pathway consists of 21 genes that maintain genomic stability and prevent cancer. Biallelic mutations within this network cause Fanconi anemia, an inherited bone marrow failure and cancer predisposition syndrome. Heterozygous inborn mutations in FA genes increase risk of breast/ovarian cancers, and somatic mutations occur in malignancies in non-Fanconi patients. Understanding the tumor suppressive functions of FA signaling is important for the study of Fanconi anemia, inherited cancers, and sporadic cancers.

The FA network functions as a genome guardian throughout the cell cycle. In addition to the well-established roles of FA proteins in interphase DNA replication/repair, the FA pathway controls mitosis by regulating the spindle assembly checkpoint (SAC) to ensure proper chromosome segregation. The SAC consists of several tumor suppressors, including Mad2, and SAC impairment predisposes to aneuploidy and cancer. However, the *in vivo* contribution of SAC dysfunction to malignant transformation of FA-deficient cells remains unknown. Furthermore, the mechanisms by which FA proteins regulate the SAC are unclear.

To test whether SAC dysfunction drives genomic instability and tumorigenesis in FA, we generated a novel FA-SAC model by intercrossing *Fancc-/-* and *Mad2+/-* mice. The

intercrossed mice displayed heightened aneuploidy secondary to exacerbated SAC dysfunction. Importantly, these mice were prone to developing hematologic malignancies, particularly leukemia, faithfully recapitulating the clinical phenotype of Fanconi anemia.

Upon establishing SAC dysfunction as a driver of tumorigenesis in FA, we next explored the mechanism by which FANCC regulates the SAC. We demonstrated that the mitotic kinase CDK1 phosphorylates FANCC to regulate subcellular localization and SAC function of FANCC during mitosis.

Our study highlights the essential role of compromised chromosome segregation in the development of leukemia due to impaired FA signaling. This work furthers our knowledge of FANCC signaling at the SAC, and has implications for future use of mitotic-centered therapies for FA-associated tumors.

D. Wade Clapp, M.D., Chair

TABLE OF CONTENTS

LIST OF TABLES

LIST OF FIGURES

LIST OF ABBREVIATIONS

AML	Acute Myeloid Leukemia
ANOVA	Analysis of variance
APC/C	Anaphase-promoting complex
BMDM	bone marrow-derived macrophage
BMF	Bone marrow failure
CDK1	Cyclin-dependent kinase 1
CIN	Chromosomal instability
DDR	DNA damage response
DEB	Diepoxybutane
DMEM	Dulbecco Modified Eagle Medium
DNA	Deoxyribonucleic acid
DSB	Double-strand break
EDTA	Ethylenediaminetetraacetic acid
FA	Fanconi anemia
FBS	Fetal bovine serum
FSC	Forward scatter
GFP	Green fluorescent protein
H & E	Hematoxylin and eosin
HSC	Hematopoietic stem cell
HSCT	Hematopoietic stem cell transplant
ICL	Interstrand crosslink
IFN-γ	Interferon-gamma
IMDM	Iscove's Modified Dulbecco's Medium
IHC	Immunohistochemistry
KBB	KNL1, Bub1, Bub3
KT	Kinetochore
LDMNC	Low-density mononuclear cell
MAD2	Mitotic arrest deficient 2
MCC	Mitotic checkpoint complex
MDS	Myelodysplastic syndrome
MEF	Mouse embryonic fibroblast
MMC	Mitomycin C

NEB	Nuclear envelope breakdown
NEK2	NIMA related kinase 2
ORF	Open reading frame
pHH3	phospho-Histone H3
RBC	Red blood cell
ROS	Reactive oxygen species
RT	Room temperature
RZZ	Rod, ZW10, Zwilch
SAC	Spindle assembly checkpoint
SD	Standard deviation
SEM	Standard error of the mean
SSC	Side scatter
TNF-α	Tumor necrosis factor alpha
UFB	Ultrafine bridge
ZW10	Zeste white 10

CHAPTER ONE

INTRODUCTION

Fanconi anemia: clinical features

Fanconi anemia (FA) is a complex genetic disorder of genomic instability, resulting in bone marrow failure, congenital abnormalities, and cancer predisposition in patients. FA has a reported incidence of 10 cases per 1 million people and a carrier frequency of 1:181 in the US (1). The classical clinical hallmark of Fanconi anemia is bone marrow failure (BMF), with a cumulative incidence of 90% by age 40 (2). Impaired hematopoiesis in the bone marrow can manifest in patients as pallor, anemia, frequent bruising or infections due to low blood counts. Other frequent hematologic abnormalities include myelodysplastic syndrome (MDS), and acute myeloid leukemia (AML) with or without pre-existing anemia (2). A variety of congenital abnormalities are also often seen in FA patients, including microcephaly, micropthalmia, short stature, and structural malformations of the thumbs, radii and ears (2, 3). Additionally, up to 1/3 of FA patients have physical findings consistent with VACTERL-H association (vertebral anomalies, anal atresia, congenital heart disease, trachea-esophageal fistula, esophageal atresia, renal/limb abnormalities, and hydrocephalous) (3). Notably, FA is associated with a heightened risk of cancer. The most common cancers seen in FA patients are AML and squamous cell carcinomas (head and neck and gynecological) (4).

The clinical standard for diagnosis of FA is a positive chromosome breakage test (5). This test is based on our knowledge that exposure to DNA crosslinking agents such as mitomycin c (MMC) or diepoxybutane (DEB) will cause chromosome fragmentation in

FA patient cells while having little effect on non-FA cells. Median age at diagnosis is 6.5 years (6), though FA patients may remain undiagnosed until adulthood upon onset of malignancy (7, 8). The vast clinical heterogeneity of this disease (**Fig. 1**) makes it likely that FA is under-diagnosed.

Management for FA patients has drastically improved with our increasing knowledge of disease pathogenesis, though median overall survival is still only 33 years (4). Progressive BMF may require an allogeneic hematopoietic stem cell transplant (HSCT). Because of sensitivity to chemotherapeutic agents and graft-versus-host disease, FA patients experience high toxicity with standard conditioning regimens prior to transplant (6), and thus transplants must be tailored. Gene therapy may also be a future option with clinical trials underway (9).

Fanconi anemia: genetics

The underlying genetics driving a diagnosis of FA are as complex as its clinical presentation. Swiss pediatrician Guido Fanconi published a case report of a family with three children with congenital abnormalities and anemia who all died young. Dr. Fanconi was the first to identify this strange constellation of symptoms as one disease, which became known as Fanconi anemia (10). It was not until the early 1990s that the *FANCC* gene was first discovered and cloned (11, 12), and cloning of the FA core complex genes *FANCA*, *FANCG*, *FANCE*, and *FANCF* soon followed (13-17). Importantly, both *BRCA1* (also known as *FANCS*) and *BRCA2* (also known as *FANCD1*) of the breast/ovarian cancer susceptibility pathway have been characterized as FA genes (18-20). With now 21

known FA genes, including the identification of *UBE2T/FANCT* (21-23), *REV7/FANCV* (24), and *XRCC2/FANCU* (25) all discovered in the last few years, work into defining the FA pathway and its functions has exploded.

Biallelic inactivation of any of the FA genes causes the disease Fanconi anemia; however, genetic disruption of the FA pathway is also seen in broader patient populations as well. Germline heterozygous FA mutation carriers have an increased risk of developing cancer. Cancer risk by age 70 for *BRCA1/FANCS* mutation carriers is estimated at 65% for breast cancer and 39% for ovarian cancer (26). Similarly, *PALB2* (*FANCN*) is both a breast cancer and pancreatic cancer susceptibility gene (27, 28). In addition to inherited cancer risks in germline FA mutations, somatic mutations and epigenetic silencing of FA genes are common in sporadic cancers, such as pancreatic cancer and squamous cell carcinomas (29-31). Understanding the tumor suppressive functions of the FA pathway (**Fig. 2**) is then important for furthering our knowledge of Fanconi anemia, inherited cancers, and cancers with sporadic mutations in FA genes.

Fanconi anemia: cellular features

Underlying the clinical and genetic heterogeneity of this disease is a unifying problem of genomic instability (**Fig. 1**). The FA pathway members have been dubbed the "guardians of the genome" for their diverse role in protecting the cell's genomic integrity from genotoxic insults. In its most studied role, the FA pathway functions in a DNA repair network during interphase to recognize and repair interstrand crosslinks (ICLs) through homologous recombination. Briefly, FANCM recognizes ICL lesions in DNA and serves

as a homing platform for the binding of the FA core complex (FANCA, FANCB, FANCC, FANCE, FANCG, FANCL, FANCM, FANCT, FAAP100, MHF1, MHF2, FAAP20 and FAAP24). The core complex serves as an ubiquitin ligase to mono-ubiquitinate FANCD2 and FANCI, thereby recruiting endonucleases and facilitating homologous recombination (Rev. in (32, 33)).

In addition to their role in repairing double-strand break (DSB) DNA damage when it occurs, there is mounting evidence that the FA pathway prevents cellular harm from replication stress and reactive oxygen species. The FA pathway stabilizes stalled replication forks during interphase, preventing fork collapse and DSB break formation, and further protecting genomic integrity (32). FA genes also insulate the promoters of antioxidant defense genes from oxidative damage (34), and exposure to oxidative stress spurs apoptosis of FA-deficient hematopoietic cells (35). In particular, FA-deficient cells display hypersensitivity to aldehyde exposure, an endogenous source of ICLs (36). Presence of a variant non-functioning ALDH2 allele in Japanese FA patients was found to be associated with heightened BMF progression (37). FANCC is also required for autophagic clearance of viruses, and multiple FA proteins have a role in mitophagy, to decrease mitochondrial reactive oxygen species (ROS) (38).

In addition to protecting against replication/repair stress and oxidative stress, FA signaling also protects the cell from inflammatory-mediated stress. FANCC in particular protects HSCs from IFN-γ and TNF-α mediated cytotoxicity (39), and *Fancc-/-* murine hematopoietic progenitor cells demonstrate hypersensitivity and increased apoptosis upon

exposure to inflammatory cytokines (40, 41). This cellular hypersensitivity, coupled with the fact that FA patient hematopoietic cells express high levels of IFN-γ and TNF-α (42), creates a toxic "cytokine storm" cellular environment.

Evidence is accumulating to support the notion of the FA pathway members as guardians of the genome, not only for their protective roles in interphase, but also for proper execution of mitosis. During mitosis, certain FA proteins localize to various parts of the mitotic apparatus, including the centrosome, spindle, and mitotic kinetochore (43, 44). In early mitosis, centrosomes serve as the spindle poles to anchor the developing spindle and microtubules undergo a "search and capture" process to capture the chromosomes and attach them to the spindle in the proper orientation. The FA pathway has been recently implicated in maintenance of centrosomal integrity upon the observation of centrosome amplification upon loss of various FA proteins (45-48). Phosphorylation of FANCA by the mitotic kinase NEK2 protects centrosomal integrity (46), and BRCA2/FANCD1 works in concert with centrosomal proteins NPM and ROCK2 to regulate centrosome number (47). In the context of DNA damage, FANCJ recruits BRCA1/FANCS and PLK1 to the centrosome to prevent centrosome amplification (48). Increased centrosome number can result in abnormal kinetochore-microtubule attachments and chromosome missegregation (49). As kinetochore-microtubule attachments form and chromosomes align, the spindle assembly checkpoint (SAC) is activated to delay anaphase until all chromosomes have been properly attached to the mitotic spindle. A functional SAC is necessary to ensure proper chromosome segregation, and the majority of the FA proteins have been shown to regulate SAC

function (43). Impairment of the SAC results in aneuploidy due to chromosome missegregation and promotes cancer (50), and accordingly, FA pathway-deficient cells demonstrate defective SAC function and aneuploidy (43, 44) (**Fig. 3**). Upon onset of anaphase, some FA proteins act to resolve ultrafine anaphase bridges (UFBs), which are abnormal structures thought to have formed from unresolved replication errors (51-53). Additionally, an intact FA pathway is necessary for proper cytokinesis. The presence of chromatin at the site of cytokinetic cleavage (due to chromosome missegregation) can block cytokinesis (54). FA pathway-deficient cells fail to complete cytokinesis (53, 55-57), and certain FA proteins, such as FANCC and BRCA2, localize to the cytokinetic midbody (43, 56). Thus the FA pathway functions at many phases throughout mitosis to preserve genomic integrity and ensure mitotic fidelity.

Aneuploidy is known to be both a cause and consequence of cancer (reviewed in (50)). As early as 1914, Theodor Boveri proposed that aneuploid cells are the founding cells of tumors, describing his hypothesis that "the primordial tumorigenic cell…is a cell that harbours a specific faulty assembly of chromosomes as a consequence of an abnormal event" (58). Chromosomal instability (CIN) refers to an ongoing change in the chromosomal makeup over rounds of division. As chromosomal makeup changes over time, cells can acquire alterations in their transcriptome and proteome that allow for a proliferative advantage, such as the loss of a tumor suppressor, and promote tumorigenesis. While aneuploidy is observed to be extremely common among cancer cells, it also can cause proliferative disadvantage and p53 activation (reviewed in

(59). This “aneuploidy paradox” is parallel to the disease scenario of Fanconi anemia, a disease of BMF and heightened cancer predisposition.

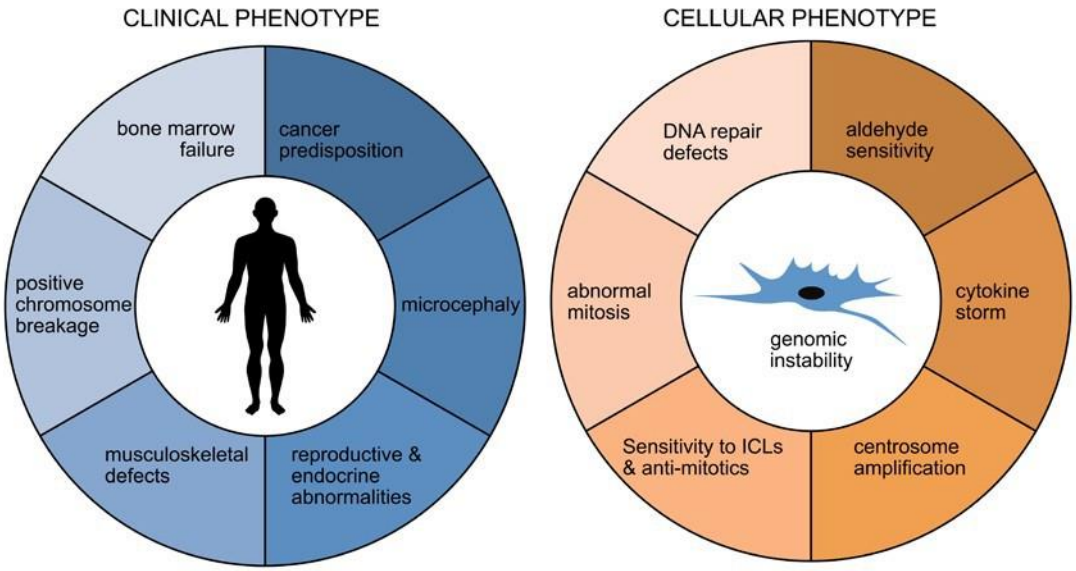

Figure 1. The FA clinical phenotype (left) and the FA cellular phenotype (right) are highly complex.

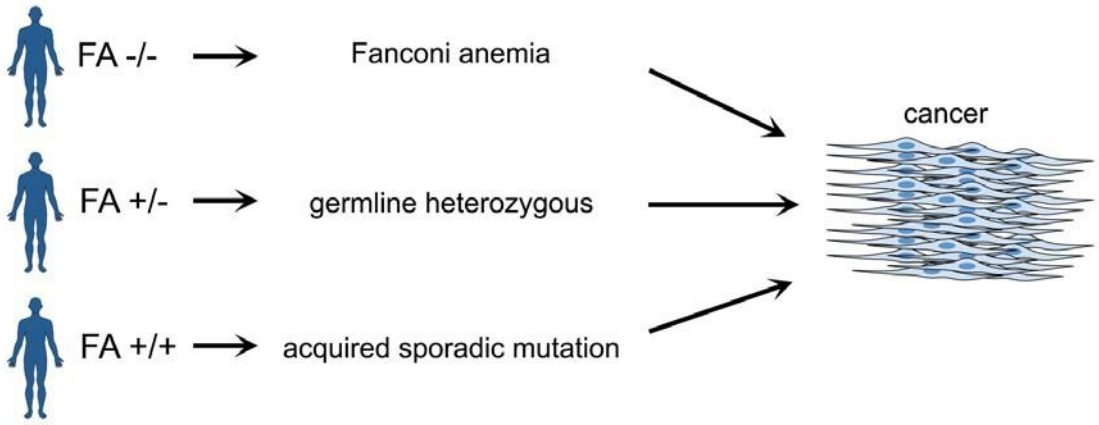

Figure 2. Bilallelic inactivation, germline heterozygosity, or somatic mutations in FA can all contribute to cancer predisposition.

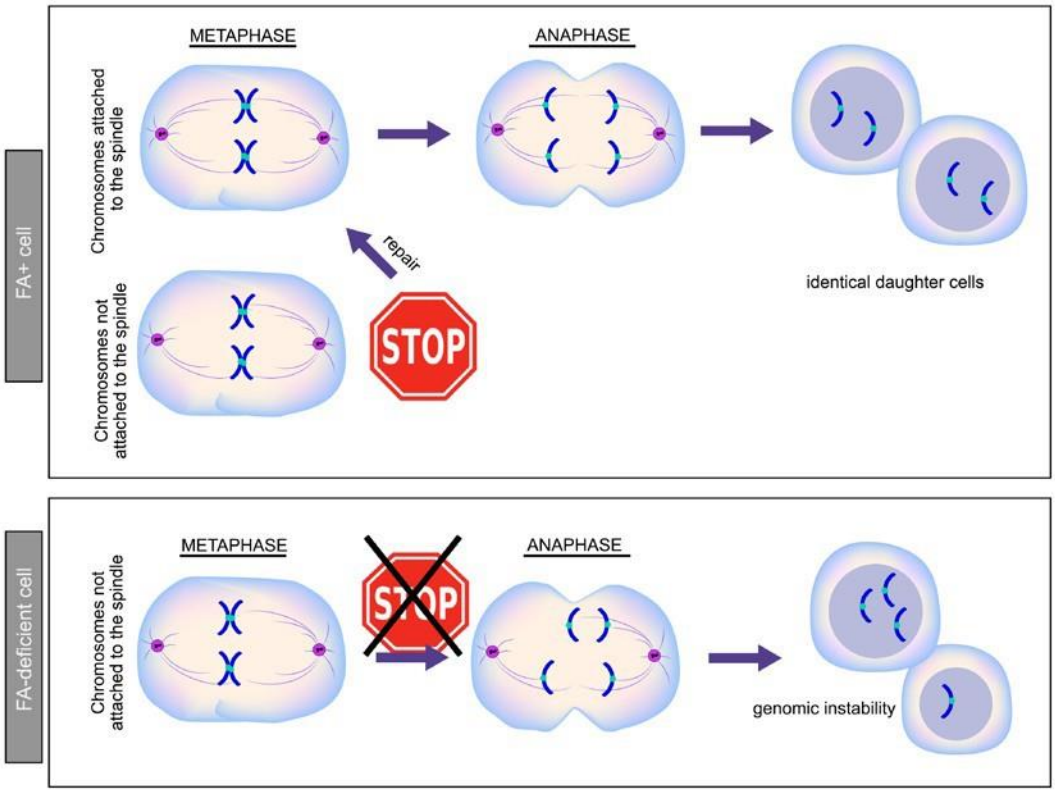

Figure 3. The SAC acts as a "halt signal" delaying anaphase until all chromosomes are properly attached to the mitotic spindle. In FA-deficient cells, the SAC is dysfunctional, promoting genomic instability.

Mouse models of FA

Our knowledge of the FA pathway family members as guardians of the genome has informed our understanding of FA disease pathogenesis. Much of our knowledge of FA disease pathogenesis comes from the use of *in vivo* murine models. Single gene knock out models exist for most of the FA pathway genes and have been well characterized (reviewed in (60)). *Brca1/Fancs* knock out mice, generated by a hematopoietic-driven Cre, demonstrate genomic instability, bone marrow failure and develop hematologic malignancies (61). Single gene knockouts of FA core complex genes, however, while effective in capturing the cellular and molecular FA phenotypes, overall do not robustly model the clinical phenotype seen in patients. *Fanca-/-*, *Fancc-/-* and *Fancg-/-* single gene knock-out mice show decreased fertility, yet do not develop BMF or heme malignancies within the first year of life (62-64). A modest fraction of aged *Fancc-/-* mice do spontaneously develop leukemias/lymphomas (65).

Instead, intercrosses of mice lacking different FA genes with mice lacking other genes as well as pharmacologic challenge of single FA gene KO models have provided great mechanistic insight and overall more effectively modeled FA cancer and BMF predisposition. *Fancc-/-*,*Fancg-/-* mice develop spontaneous BMF and AML and have genomic instability (66), suggesting that certain FA genes may have cooperative tumor suppressive roles. However *Fancc-/- Fanca-/-* mice are phenotypically identical to single knockouts (67), providing evidence that certain individual FA genes are functionally epistatic with each other.

Mouse models have demonstrated that DNA damage can drive disease in a FA-deficient background. MMC treatment sparks BMF in *Fancc-/-* mice (68). Ionizing radiation induces p53 expression in *Fancc-/-* mice, and loss of both *Fancc* and *p53* accelerate tumorigenesis in a murine model (69). Likewise, *p53* heterozygosity accelerates tumorigenesis in *Fancd2-/-* mice (70).

Multiple recently developed mouse models have demonstrated the protective role of FA signaling in the face of oxidative stress. Mice deficient for both *Fancc* and *Sod1*, a superoxide-detoxifying enzyme, exhibit impaired hematopoiesis in the context of increased reactive oxygen species (ROS) (71). *Aldh2-/-Fancd2-/-* mice spontaneously develop leukemias and acetyaldehdye exposure causes BMF secondary to DNA damage in *Aldh2-/- Fancd2-/-* mice (72). Aged *Aldh2-/-Fancd2-/-* mice spontaneously develop BMF, and demonstrate decreased numbers of hematopoietic stem cells (HSCs) and DNA damage in the HSCs (73). Interestingly, treatment with the diabetes drug metformin, which can mitigate aldehyde toxicity, increased the frequency of HSCs in *Fancd2-/-* mice and delayed tumorigenesis in *Fancd2-/-, p53+/-* mice (74). Taken together, these studies demonstrate that oxidative stress causes BMF and leukemogenesis in FA *in vivo*.

Mouse models have also furthered our understanding of the *in vivo* signaling that occurs upon loss of FA and drives BMF. In response to replicative stress and DNA damage, p53 is hyperactivated in FA cells and triggers G0/G1 cell cycle arrest, leading to exhaustion of the HSC pool and BMF (75). Hyperactive TGFbeta signaling is also contributory to HSC impairment in FA. Inhibiting TGFbeta signaling rescues the functional defects of

HSCs from *Fancd2-/-* mice and rescues physiological stress-induced BMF (76). Another mechanism driving BMF in FA murine models is inhibitory cytokine hypersensitivity and apoptosis of *Fancc-/-* hematopoietic progenitors (40).

While models exist to understand the contribution of various interphase roles of FA signaling as *in vivo* guardians of the genome, little work has been done to investigate whether abnormal mitosis upon loss of FA signaling could contribute to disease *in vivo*. Work by Choi et al (2012) has uncovered a role for BRCA2/FANCD1 in facilitating acetylation of the kinetochore protein BubR1 to regulate the SAC, and demonstrated that a mouse model lacking BRAC2-BUBR1 binding ability spontaneously develops various tumors and genomic instability (77, 78). This is a promising lead, however, it remains unknown whether the FA core complex members, such as FANCC, modulate the SAC to prevent tumorigenesis. Also there is a need for an FA-SAC model that more closely resembles the hematopoietic-specific diseases of FA patients.

There is still a great need for targeted therapies for FA patients and patients with FA-deficient cancers. Recent evidence demonstrates that FA signaling regulates the SAC, and SAC dysfunction is a known cause of malignancy. However, the *in vivo* significance of SAC dysfunction in FA signaling remains unclear. Thus we set out to establish a new FA-SAC mouse model to 1) test whether SAC dysfunction can drive genomic instability and tumorigenesis in FA *in vivo*, and 2) provide a rationale to explore new mitotic-centered therapies for FA-associated malignancies. We genetically weakened the SAC in the FA-deficient background by generating *Fancc-/-;Mad2+/-* intercrossed mice. *Mad2* is

a tumor suppressor well known for its role in regulating the SAC (79) without directly affecting interphase DNA damage repair. *Mad2* heterozygosity in the *Fancc-/-* background allows us to further impair only one pathway (SAC) out of the multiple tumor suppressor networks (such as SAC and DDR) affected by loss of FA signaling, in order to determine whether SAC dysfunction drives tumorigenesis in the context of FA.

MATERIALS AND METHODS

Mice

Mad2+/- and *Fancc-/-* mice (C57Bl/6J background) were a gift of D. Wade Clapp (Indiana University). Mice were genotyped via PCR as previously described (66). B6.SJL-*PtprcaPepcb*/BoyJ mice were purchased from the Indiana University In Vivo Therapeutics Core. All studies were performed in accordance with the policies of the institutional animal care and use committee of Indiana University.

Peripheral blood assays

Peripheral blood was drawn from the lateral tail vein and collected into EDTA-coated collection tubes. Complete blood counts were obtained using a Hemavet 950FS (Drew Scientific). Blood was smeared onto slides, stained with Geisma, and imaged using a Zeiss Axiolab microscope.

For chimerism analysis, peripheral blood was collected monthly post-transplant as described above. Cells were stained with anti-CD45.2-FITC (BD Biosciences) and anti-CD45.1-PE (BD Biosciences) as previously described (66), and analyzed on a FacsCalibur machine (Becton-Dickinson). For lineage classification of WBCs, the following antibodies were used: anti-CD3e (BD Bioscience), anti-B220 (clone RA3-6B2, BD Pharmingen), anti-cd11b (clone M1/70, eBioscience), anti-Ly-6G/Ly-6C (clone RB6-8C5, Biolegend). At least 10,000 events per sample were acquired. Data was analyzed using FlowJo Software.

Bone marrow transplantation

For competitive repopulation studies, $1.5x10^6$ donor test LDMNCs (C57Bl/6J background) and 1.5x106 donor competitor LDMNCs (BoyJ background) were transplanted into each recipient mouse via tail vein injection. Recipients were 8 week-old female B6.SJL-*PtprcaPepcb*/BoyJ mice that underwent whole-body split-dose 1100 rads irradiation (700 rads/400 rads, 4 hours apart). For transplant of leukemic marrows, 0.5-1 million donor cells were transplanted into lethally irradiated recipient female B6.SJL-*PtprcaPepcb*/BoyJ mice with CD45.1+ *wt* competitor cells at a ratio of 1:1 or 1.4:1 donor:competitor.

Bone marrow harvesting

Bone marrow cells were flushed from tibias and femurs of mice using a 23-gauge needle and syringe (Becton Dickinson). LDMNCs were isolated by density gradient using Histopaque-1119 (Sigma), centrifuging for 30 minutes at 1800rpm with no brake. After centrifugation, LDMNCs were removed from the interface layer and either utilized for transplantation or culturing. Murine cytospins were made by resuspending LDMNCs in PBS and centrifuging onto slides at 450rpm for 5 minutes on a Shandon Cytospin 3 Cytocentrifuge (Thermo Scientific).

Histology

Tissues collected from mice post-mortem were fixed in 10% formalin and subsequently embedded in paraffin, sectioned (5uM sections), and stained with hematoxylin and eosin (H & E). The following antibodies were used for immunohistochemistry staining: anti-

ckit (C19, Santa Cruz, 1:50), anti-cd11b (Novus Biologicals, 1:50), CD3 (Dako IR503), B220 (Clone RA3-6B2, BD-550286). Peripheral blood smears and bone marrow cytospins were stained with Geisma using the automated Siemens Hematek 3000 (Fisher) system.

Diagnoses of leukemia and lymphoma were made using criteria established in the Bethesda proposals for classification of nonlymphoid neoplasms in mice (80), and the Bethesda proposals for classification of lymphoid neoplasms in mice (81). Diagnoses were confirmed by a hematopathologist at IU School of Medicine.

Hematopoietic progenitor assay

20,000 LDMNCS were plated in triplicate onto 35x10mm culture dishes with 2mm grids (Thermo Scientific) and grown in methycellulose (H4100 STEMCELL) media in IMDM containing the following: 100ng/ml m-SCF, 10ng/ml mGM-CSF, 5ng/ml mIL-3, 4 units/ml EPO, 20mM glutamine, 0.00005% βME, 30% FBS, 1% P/S and MMC at indicated concentrations. The cells were incubated at 37^{o}C and 5% CO_2 for 7 days and then scored. A colony was defined as a cluster of ≥50 cells.

Metaphase spreads

Bone marrow cells flushed from tibias were cultured in IMDM supplemented with 20% FBS, murine stem cell factor (100ng/ml), and IL-6 (200ng/ml) for 2 days. Cells were then exposed to 0.2ug/ml colcemid (Life Tech) for 4 hours and pelleted at 800 rpm for 5 minutes. Cells were resuspended dropwise in pre-warmed (37^{o}C) 75mM KCl while

vortexing gently, and incubated at 37ºC for 15 minutes. After pelleting, cells were resuspended in a 3:1 methanol: glacial acetic acid fixative solution. Cells were pelleted and resuspended in fixative solution two additional times before being dropped onto slides and dried overnight. Spreads were then stained with Vectashield mounting medium with Dapi (Vector Laboratories). For the chromosome breakage test, cells were cultured for 48 hours in 50nM MMC before addition of colcemid. For spectral karyotyping (SKY), samples were prepared as above and imaged and analyzed by the MD Anderson Cancer Center Molecular Cytogenetics Facility.

SAC escape imaging studies

Ckit+ cells were isolated from LDMNC population by MACs sorting (mouse CD117 magnetic beads, Miltenyi Biotec), and cultured for 24 hours in 10% FBS, 1% P/S, 100ng/ml TPO, 100ng/ml SCF, and 100ng/ml Flt3 in RPMI media. The cells were then pulsed with 10uM EDU for 2 hours, followed by treatment with 100ng/ml nocodazole for 12 hours. Cell fixation and EDU staining was performed using the Click-it Edu imaging kit (Thermo scientific), followed by staining with pHH3 antibody conjugated to Alexa 647 (Cell signaling, 1:50). Cells were spun onto coverslips via cytospin at 450rpm for 5min, and then mounted onto coverslips with ProLong Diamond Antifade mountant with Dapi (Thermo). EDU+ cells were counted on the deconvolution microscope at 100x. BMDMs were obtained by culturing the LDMNCs in IMDM supplemented with 20% FBS, 10ng/ml M-CSF, and 1%P/S for 7 days.

Microscopy

Images of murine blood smears, cytospins, and histological sections were obtained using a Zeiss Axiolab microscope containing a color camera.

Images of metaphase spreads were acquired on a Deltavision personalDx deconvolution microscope (Applied Precision) furnished with 20x, 60x, 100x and a CCD camera. Image stacks (distance between z-sections: 0.2μm) were deconvolved using Softworx software suite (10 iterations; ratio: conservative) and analyzed using Imaris software suite (Bitplane). For observation of duration of mitosis, a Biostation IMQ live imaging microscope (Nikon) with a z220 workstation (Hewlett Packard) and an attached 37ºC incubator was used. Phase contrast image stacks (distance between z sections: 2 μm) were captured in two-minute intervals for up to 24 hours. Videos were analyzed using NIS-Elements Viewer software.

RESULTS

Genetic disruption of *Fancc* and *Mad2* cooperate to promote hematologic malignancies

Fancc-/- mice are viable with a mild impairment in the SAC (44) and develop cancer late in life (60, 63, 68). *Mad2-/-* mice are embryonic lethal due to severe aneuploidy (82), while *Mad2+/-* mice display only a mild predisposition for tumorigenesis late in life and modestly impaired SAC function (79). If error-prone chromosome segregation contributes to leukemogenesis in FA, *Fancc-/-; Mad2+/-* mice should be more prone to cancer than age-matched *wt*, *Fancc-/-*, and *Mad2+/-* animals (**Fig. 4**).

Due to known impaired fertility of the *Fancc-/-* genotype, we crossed *Fancc+/-* mice with *Fancc+/-; Mad2+/-* mice to obtain *Fancc-/-; Mad2+/-* mice. Importantly, a 24-month observation study of cohorts of *Fancc-/-; Mad2+/-* mice alongside *wt; Mad2+/-;* and *Fancc-/-* cohorts revealed shortened life span of *Fancc-/-; Mad2+/-* animals (**Fig. 5B**, $p < 0.0001$). These mice were dying prematurely due to hematologic malignancies (**Table 1**), mainly myeloid leukemias (**Fig. 6**). Moribund *Fancc-/-; Mad2+/-* mice were diagnosed with myeloid leukemia according to Bethesda criteria ((80), **Fig. 7**). These mice had splenomegaly (**Fig. 6A**), and a predominance of blasts (**Fig. 6B**) and myeloid cells expressing lineage surface markers Gr1 and Mac1 in the peripheral blood (**Fig. 6C-D**). We also observed myeloid cell infiltrates into the liver and spleen, and increased ckit+ staining by bone marrow immunohistochemistry, suggestive of an expansion of precursor cells in the marrow (**Fig. 6E**). Importantly, transplant of leukemic *Fancc-/-; Mad2+/-* bone marrow cells to healthy irradiated recipients was lethal to recipient mice. Recipients displayed a myeloid skewing in the peripheral blood, leukemic liver

infiltrates, and myeloid takeover of the bone marrow similar to disease presentation in the donor mouse (**Fig. 8, Table 2**). Additionally, a subset of *Fancc-/-; Mad2+/-* mice, particularly >1 year of age, died of lymphoid leukemia/lymphoma. These mice had large abdominal masses containing lymphoid cells, CD3+ or B220+ hematopoietic infiltrates in the liver, and an unusual population of CD3low+B220low+ cells in the peripheral blood (**Fig. 9**).

Sick *Fancc-/-; Mad2+/-* mice also displayed additional hematologic abnormalities, including cytopenias, decreased bone marrow cellularity, and decreased colony forming potential in methylcellulose progenitor assays (**Fig. 10**). Interestingly healthy 2-3 month old *Fancc-/-; Mad2+/-* mice do not display these abnormalities, and have blood counts, cellularity and progenitor function comparable to age-matched *wt* or single mutant (*Fancc-/-* or *Mad2+/-*) mice until acute disease (**Fig. 10**).

To study in further detail specifically the malignant potential of *Fancc-/-; Mad2+/-* hematopoietic cells, we performed competitive repopulation transplant experiments. Bone marrow test cells (CD45.2+) from *Fancc-/-; Mad2+/-* mice or controls (*wt; Fancc-/-;* or *Mad2+/-*) were transplanted into lethally-irradiated *wt* recipients along with *wt* competitor (CD45.1+) cells (**Fig. 11A**). After transplantation, peripheral blood CD45.2 vs CD45.1 chimerism was compared monthly to determine the ability of the donor test cells to outcompete competitor cells and stably reconstitute hematopoiesis in the recipient marrows.

Post transplant, individual recipient mice that received the genomically unstable *Fancc-/-; Mad2+/-* hematopoietic stem cells displayed a wide variation (Bartlett's test, p=0.0178) in chimerism, while recipients of control test cells (*wt; Mad2+/-* or *Fancc-/-*) showed similar levels of chimerism among individual recipients (**Fig. 11B**). Additionally, by 1 year post-transplant, the transplanted CD45.2+ *Fancc-/-; Mad2+/-* cells were producing WBCs that were predominantly myeloid, as assessed by flow cytometry of peripheral blood for lineage markers CD11b, Gr-1, CD3, and B220 (**Fig. 11C-D**), suggestive of clonal evolution in these animals. Indeed, MDS was found in 64.3% of *Fancc-/-; Mad2+/-* recipients at time of necropsy, as compared to 0% of recipients of *wt, Mad2+/-* or *Fancc-/-* marrow (**Fig. 11E**). CD45.2+ *Fancc-/-; Mad2+/-* donor test cells showed impaired colony-forming ability in methycellulose assays (**Fig. 11F**), indicating impaired HSC function. The findings of varied recipient chimerism, MDS post-transplant and functional impairment in *Fancc-/-; Mad2+/-* HSCs supports the notion that deficiency of these two SAC regulators cooperates to disrupt proper hematopoiesis.

Thus we have established a novel FA mouse model that reflects the FA clinical manifestations of cancer predisposition (particularly leukemias) and impaired hematopoiesis due to impaired SAC.

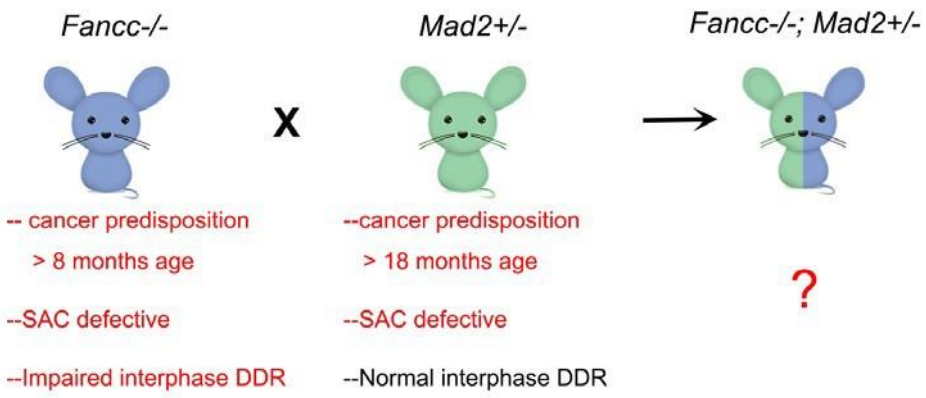

Figure 4. Schematic of *Fancc-/-; Mad2+/-* intercross detailing known phenotypes of single gene mutant mice.

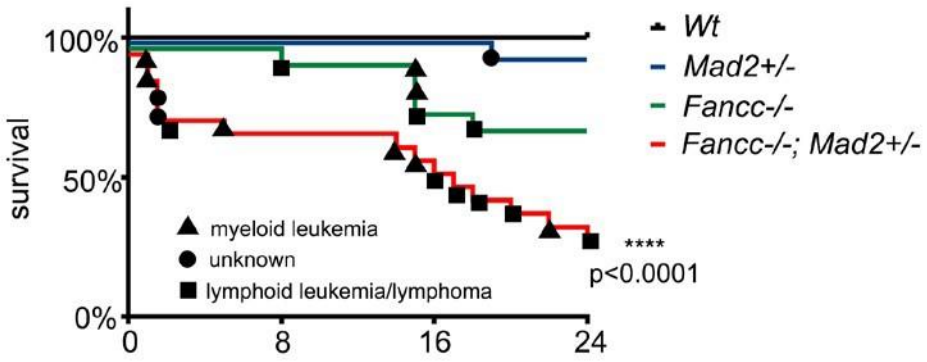

Figure 5. *Fancc-/-; Mad2+/-* mice have shortened life span and succumb to hematologic malignancies. The p value at 24 months was calculated by log rank Mantel-Cox test ($n \geq 17$ mice/genotype). Symbols represent individual diagnoses at time of death.

Summary of *Fancc-/-; Mad2+/-* individual moribund mice with hematologic malignancies			
Mouse ID	**Days lived**	**Disease findings**	**Diagnosis**
887	33	leukocytosis, monocytosis, blasts in PB and BM	myeloid leukemia
846	36	anemia, blasts in PB and BM, hypocellular marrow	myeloid leukemia
204	139	anemia, splenomegaly, cd11b+ liver and spleen infiltrates	myeloid leukemia
233	420	anemia, monocytosis, liver and spleen infiltrates, disease transplantable to irradiated recipients	myeloid leukemia
99	670	pancytopenia, splenomegaly, blasts in PB and cytospin, Gr1+cd11b+ cells in PB, disease transplantable to irradiated recipients	myeloid leukemia
504	465	anemia, monocytosis, splenomegaly, liver and spleen infiltrates, blasts in PB, hypocellular marrow, disease transplantable to irradiated recipients	myeloid leukemia (sub- classification: histiocytic sarcoma)
251	44	pancytopenia, blasts in PB	unknown*
637	42	thrombocytopenia, monocytosis, blasts in PB	unknown*
704	42	pancytopenia, hypocellular marrow, blasts in PB, increased B220 positivity in BM and PB	lymphoid leukemia
415	506	$CD3^{low+}B220^{low+}$ blasts in PB & cytospin, hypocellular marrow; disease transplanted to irradiated recipients	lymphoid leukemia
430	548	pancytopenia, hypocellular marrow, abdominal hematopoietic mass, splenomegaly, CD3+ B220+ liver and spleen infiltrates	lymphoid leukemia
145	622	pancytopenia, B220+ liver & spleen infiltrates, numerous mitotic figures in BM histology	lymphoid leukemia
420	599	CD3+ hematopoietic abdominal mass	lymphoid leukemia/lymphoma
164	730	CD3+ B220+ hematopoietic abdominal mass, liver infiltrates	lymphoid leukemia/lymphoma

Table 1. Summary of individual cases of *Fancc-/-; Mad2+/-* moribund mice with hematologic malignancies. PB = peripheral blood; BM= bone marrow. *Designation of unknown was given to cases in which leukemia was suspected, but Bethesda criteria for leukemia was not able to be fully met due to lack of evidence or decomposed tissues.

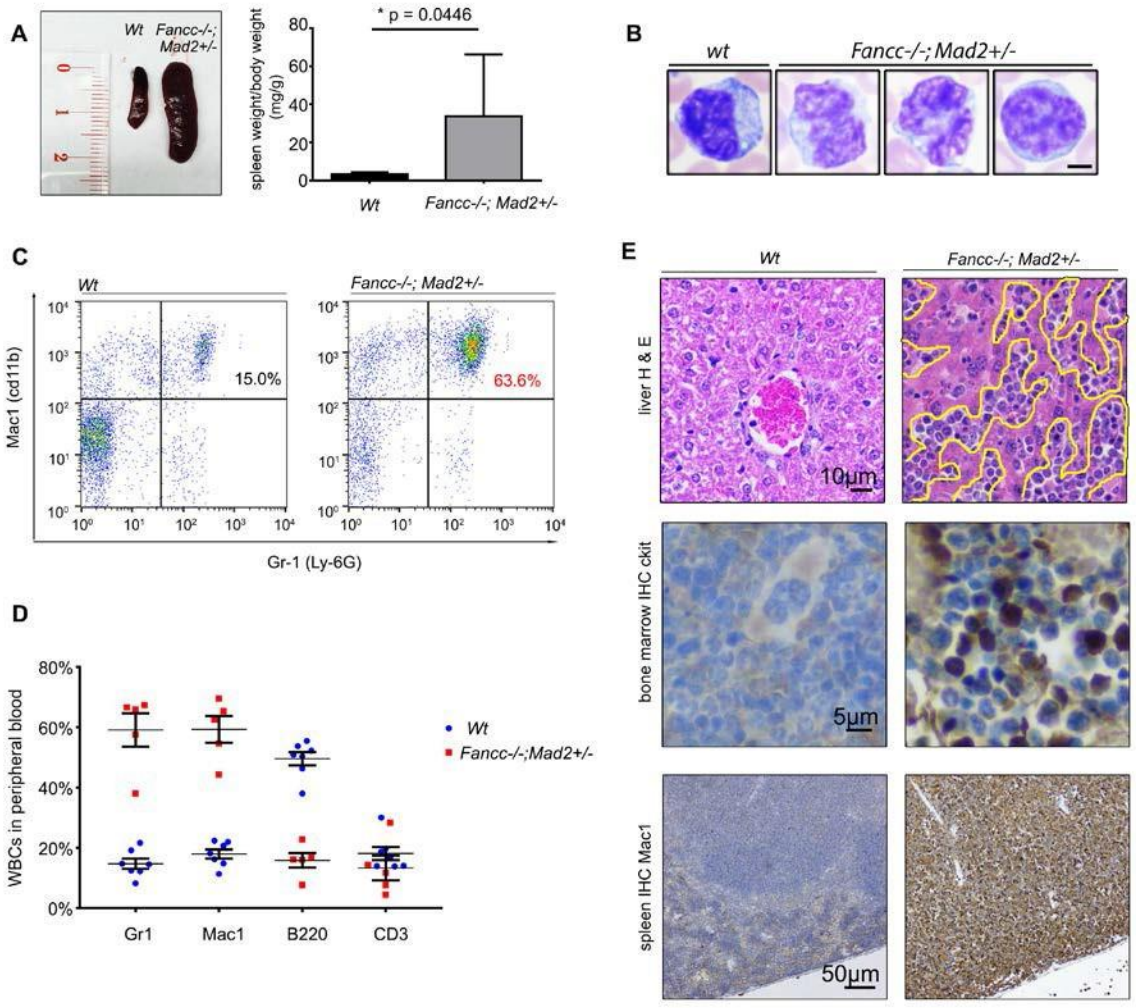

Figure 6. Myeloid leukemias in *Fancc-/-; Mad2+/-* mice. (A) Splenomegaly in the moribund *Fancc-/-; Mad2+/-* mice. Error bars represent SEM and the p value was obtained by student's t test, with n ≥ 5 mice/genotype. (B) Representative images of myeloid blasts in peripheral blood of *Fancc-/-; Mad2+/-* mice (right) compared with a *wt* monocyte. Blasts were defined according to the Bethesda criteria (80). Peripheral blood flow of moribund *Fancc-/-; Mad2+/-* mice showed a high percentage of WBCs positive for myeloid markers Gr1 and Mac1 (C, D). Quantification represents at least 5 mice per group. (E) Histological sections of *Fancc-/-; Mad2+/-* mice (right) compared with *wt* (left). Leukemic infiltrates on liver H & E (top, yellow lines outline infiltrates), ckit+ IHC

staining in bone marrow H & E (middle), and Mac1+ staining on IHC of spleen (bottom) are prominent features of the *Fancc-/-; Mad2+/-* myeloid leukemias.

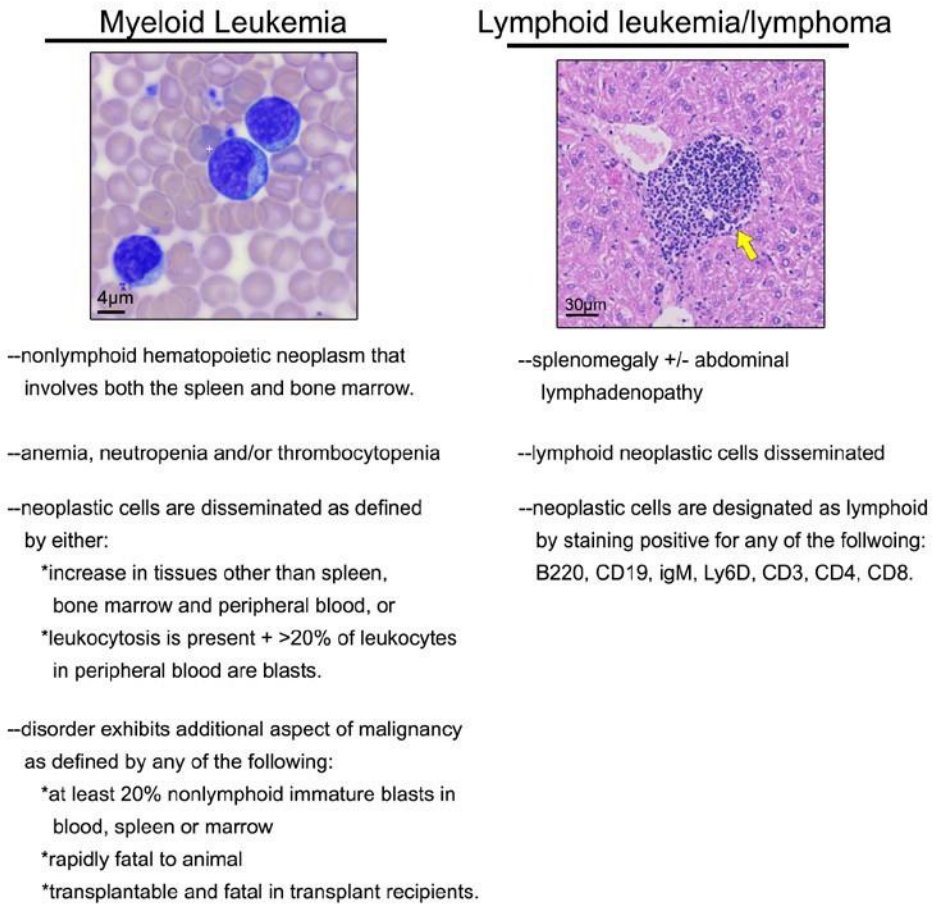

Figure 7. Summary of criteria used for diagnosis of murine hematologic illnesses. Criteria were adapted from the Bethesda proposals for classification of nonlymphoid hematopoietic neoplasms in mice (80), and the Bethesda proposals for the classification of lymphoid neoplasms in mice (81).

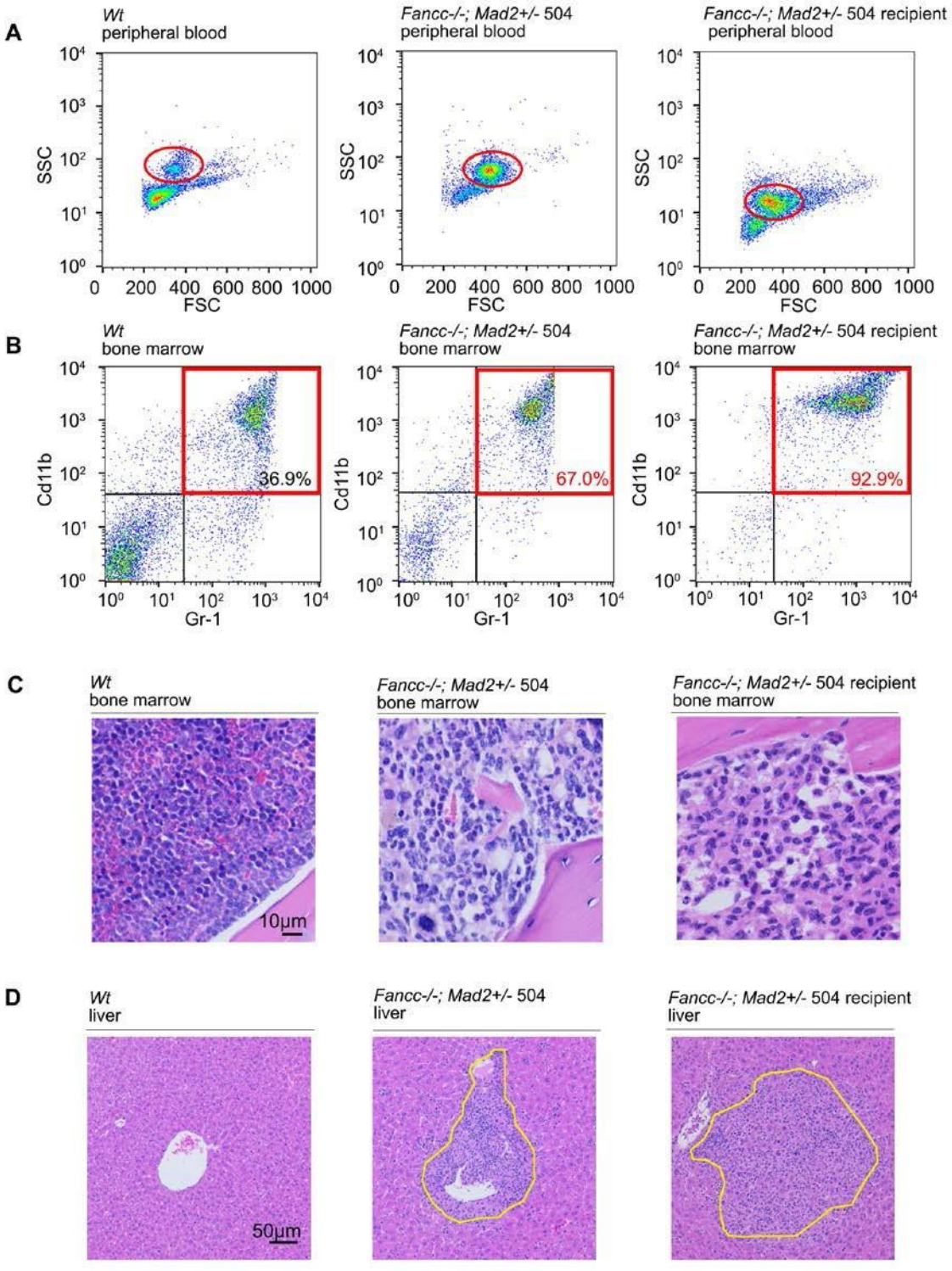

Figure 8. Leukemia from *Fancc-/-;Mad2+/-* donor resulted in disease in transplant recipients. One million LDMNCs from *Fancc-/-;Mad2+/-* #504 were transplanted into

two lethally irradiated recipients, both of which died of disease. Forward and side scatter flow profiles (A) of WBCs from peripheral blood depict a high FSC/SSC population, consistent with myeloid cells, that predominates in the 504 donor and recipient mice. (B) WBCs from bone marrow of both 504 donor and 504 recipients are predominately Gr1+Mac1+. (C) Bone marrow H & E sections from both 504 donor and recipient show a uniform myeloid population, as compared with the mixture of heterogeneous cell types seen in *wt* marrow section. (D) Liver infiltrates are evident in both 504 donor and recipient mice.

Transplantation of leukemias from *Fancc-/-;Mad2+/-* mice to healthy recipients				
Donor mouse genotype	**transplant donor:competitor ratio**	**recipient death due to leukemia**	**incidence of leukemia at end of study**	**disease classification**
Wt # 891	1:1	0/3	0/3	N/A
Wt # 726	1:1	0/2	0/2	N/A
Wt # 565	1.4:1	0/3	0/3	N/A
Fancc-/-;Mad2+/- #504	1:1	2/2	2/2	myeloid leukemia
Fancc-/-;Mad2+/- #233	1:1	2/5	5/5	myeloid leukemia
Fancc-/-;Mad2+/- #99	1.4:1	1/3	3/3	myeloid leukemia
Fancc-/-;Mad2+/- #415	1.4:1	1/2	2/2	lymphoid leukemia

Table 2. Summary of *Fancc-/-;Mad2+/-* leukemia transplants. Transplantation of leukemic bone marrow from moribund *Fancc-/-;Mad2+/-* donor mice resulted in disease in transplant recipients. Lethally irradiated recipient mice were transplanted with donor cells as well as a fraction of *wt* competitor cells to ensure recipient survival post-transplant.

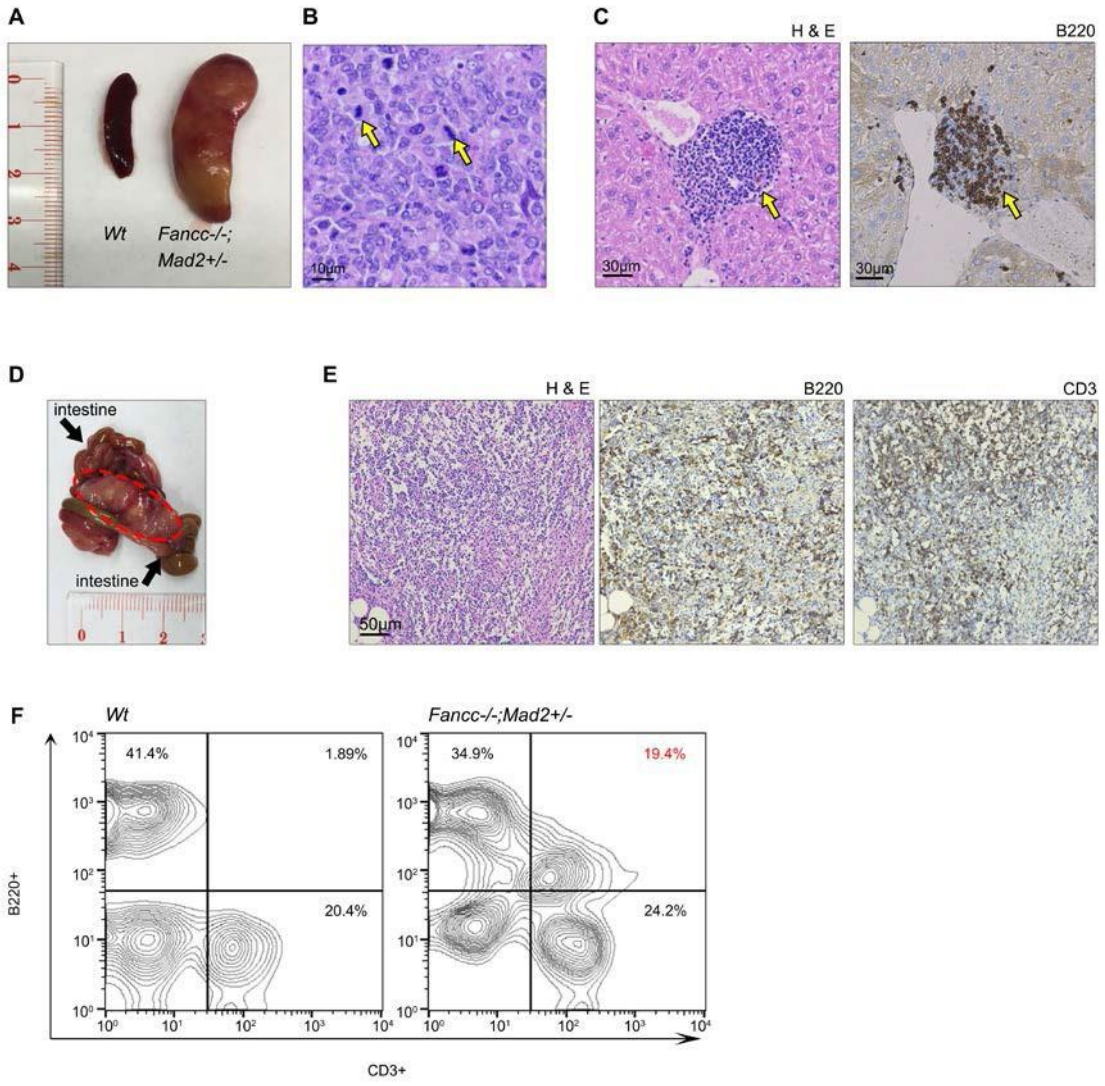

Figure 9. Lymphoid leukemia/lymphomas in *Fancc-/-; Mad2+/-* mice. Splenomegaly (A) and increased mitotic figures (yellow arrows) in splenic germinal centers (B) of *Fancc-/-; Mad2+/-* mice with follicular lymphomas. (C) Lymphoid infiltrate (yellow arrow) into liver (left) that stains positive for B cell marker B220 by IHC (right) in moribund *Fancc-/-; Mad2+/-* mouse. (D) Abdominal lymphoid mass (red dashed line) surrounding intestine of *Fancc-/-;Mad2+/-* mouse. (E) H & E (left) and IHC (right) of abdominal mass reveals CD3+ and B220+ cell populations. (F) Flow cytometry of WBCs from peripheral blood of a moribund *Fancc-/-; Mad2+/-* mouse (right), showing an

aberrant circulating population of CD3low+B220low+ cells, compared with a wt flow profile (left).

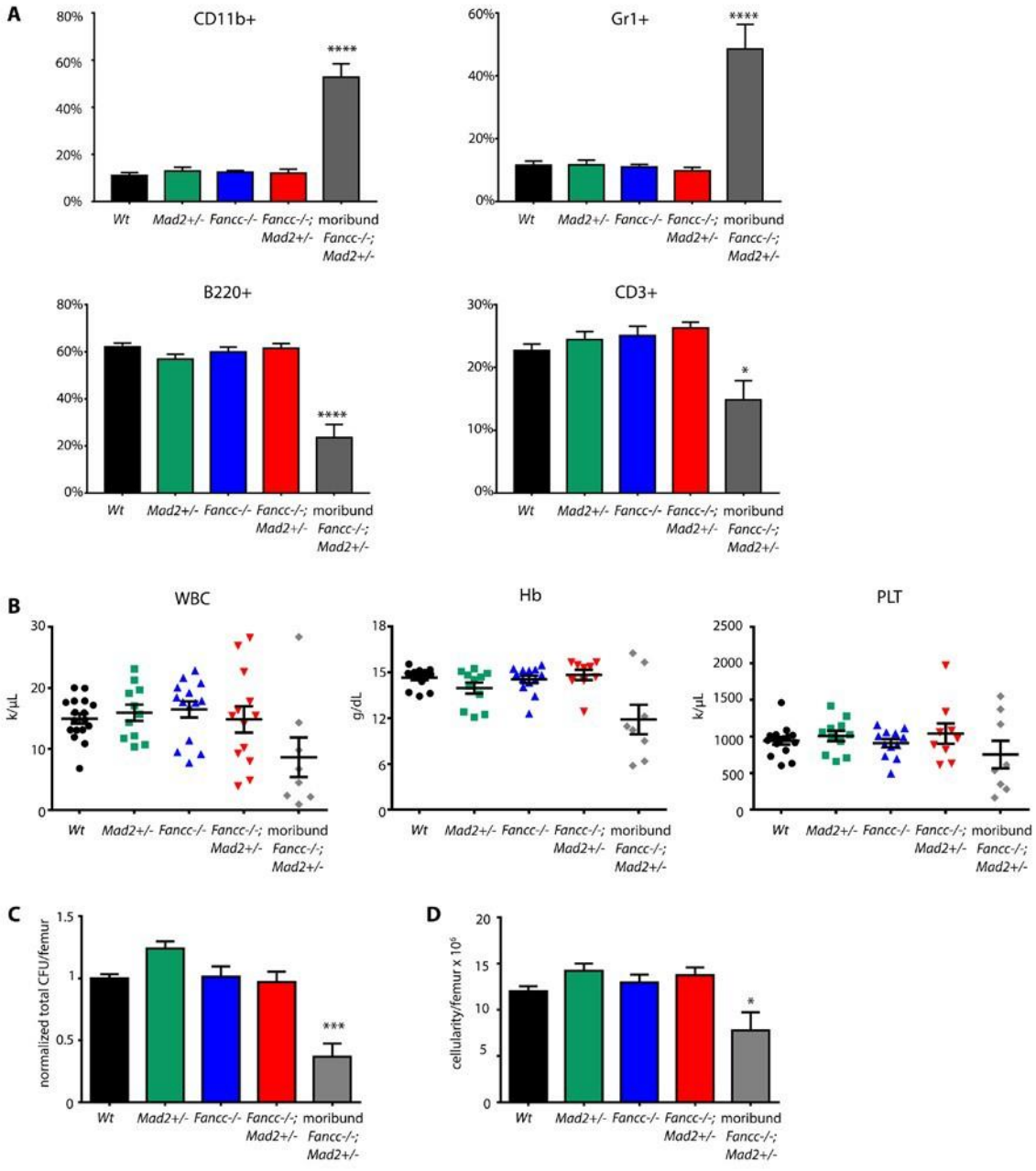

Figure 10. Normal hematopoiesis in *Fancc-/-; Mad2+/-* mice until moribund state.

(A) Percentage of WBCs expressing lineage specific surface markers from peripheral blood. 2-3 month old healthy mice of all genotypes were compared with moribund *Fancc-/-; Mad2+/-* mice at time of death, n≥5mice/group. (B) Levels of WBCs, hemoglobin, and platelets obtained from complete blood counts of 2-3 month old healthy

mice or moribund mice at time of death, n≥8 mice/group. (C) Total number of colonies grown in methylcellulose colony forming assays and (D) bone marrow cellularity of healthy 16 week old mice and moribund *Fancc-/-; Mad2+/-* mice, n≥9 mice/group. Statistics represent One-way ANOVA with Dunnett's multiple comparisons test, *$p \leq 0.05$, *** $p \leq 0.001$, **** $p \leq 0.0001$.

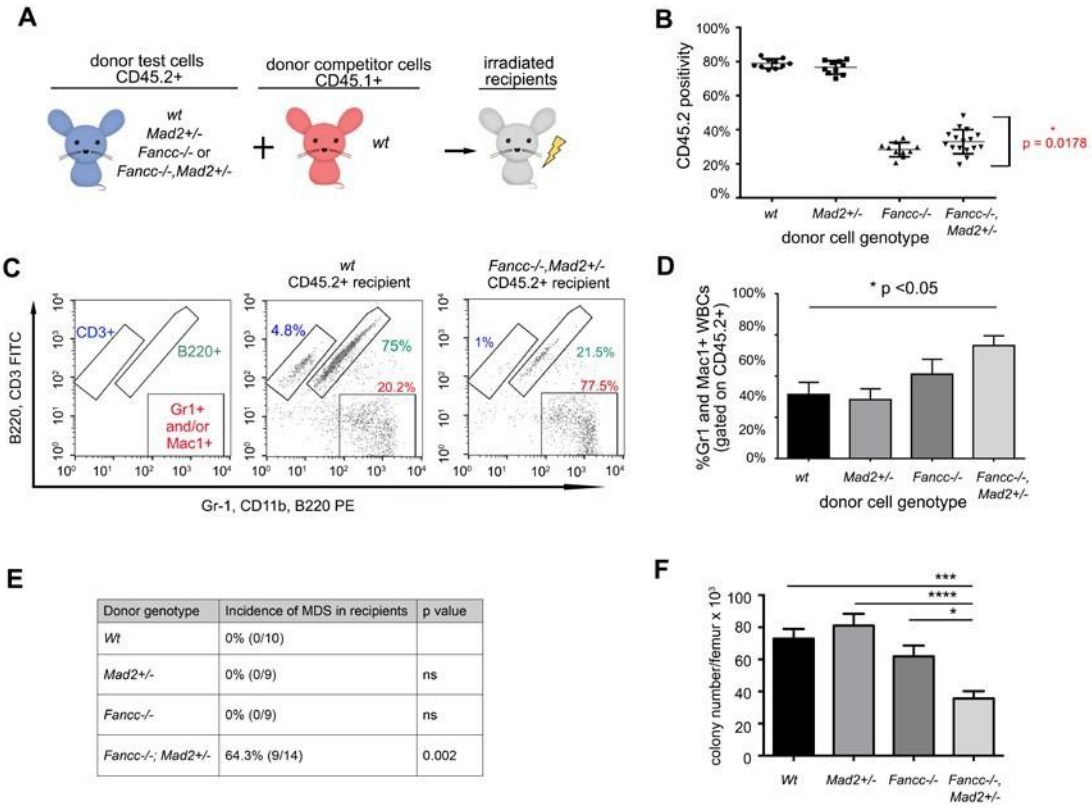

Donor genotype	Incidence of MDS in recipients	p value
Wt	0% (0/10)	
Mad2+/-	0% (0/9)	ns
Fancc-/-	0% (0/9)	ns
Fancc-/-; Mad2+/-	64.3% (9/14)	0.002

Figure 11. Competitive repopulation transplant experiment highlights malignant potential of *Fancc-/-; Mad2+/-* HSCs. (A) Transplant schema for competitive repopulation studies. (B) Peripheral blood chimerism in transplant recipients at 3 months post transplant. Error bars represent standard error of the mean, and statistics were obtained from Bartlett's test for differences in standard deviations. Representative flow profiles (C) and quantification of myeloid populations (D) in PB gated on CD45.2+, 1 year post-transplant. Graph represents at least 7 mice/group. (E) Table depicting incidence of myelodysplasia in transplant recipients 1 year after transplant. Fisher's exact test was used for statistics, with $p<0.01$ considered significant. (F) Colony forming ability of CD45.2+ cells harvested from primary recipients one-year post transplant. 20,000 LDMNCs were plated on methylcellulose in triplicate (n = 4 recipient mice/group). Error

bars represent SEM, and analysis was done via one-way ANOVA with Bonferroni's post hoc test for both (D) and (F).

Fancc-/-;Mad2+/- mice display heightened genomic instability

Due to genetic disruption of two SAC genes in *Fancc-/-; Mad2+/-* mice, we expected to observe a heighted genomic instability in this genotype to accompany the cancer predisposition phenotype. Spectral karyotyping of bone marrow cells from leukemic *Fancc-/-;Mad2+/-* mice revealed whole chromosome gains and losses (**Fig. 12A**). We also counted chromosome numbers in metaphase spreads prepared from cultured LDMNCs from healthy age-matched mice of all genotypes, and found a heightened incidence of aneuploidy in the *Fancc-/-;Mad2+/-* group (**Fig. 12B-C**). We were also able to identify exacerbated genomic instability in the *Fancc-/-; Mad2+/-* erythroid lineage using a pre-established red blood cell (RBC) micronucleation assay (44). Via flow cytometry, we identified an increased percentage of genomically unstable micronucleated RBCs (defined as CD71-, propidium iodide+) in the peripheral blood of *Fancc-/-; Mad2+/-* mice at 12 months of age compared to age-matched littermates of control genotypes (**Fig. 13A-B**). Imaging of Geisma-stained cytospins also revealed similar findings of a greater percentage of multinucleated bone marrow cells in the *Fancc-/-; Mad2+/-* mice (**Fig. 13C-D**).

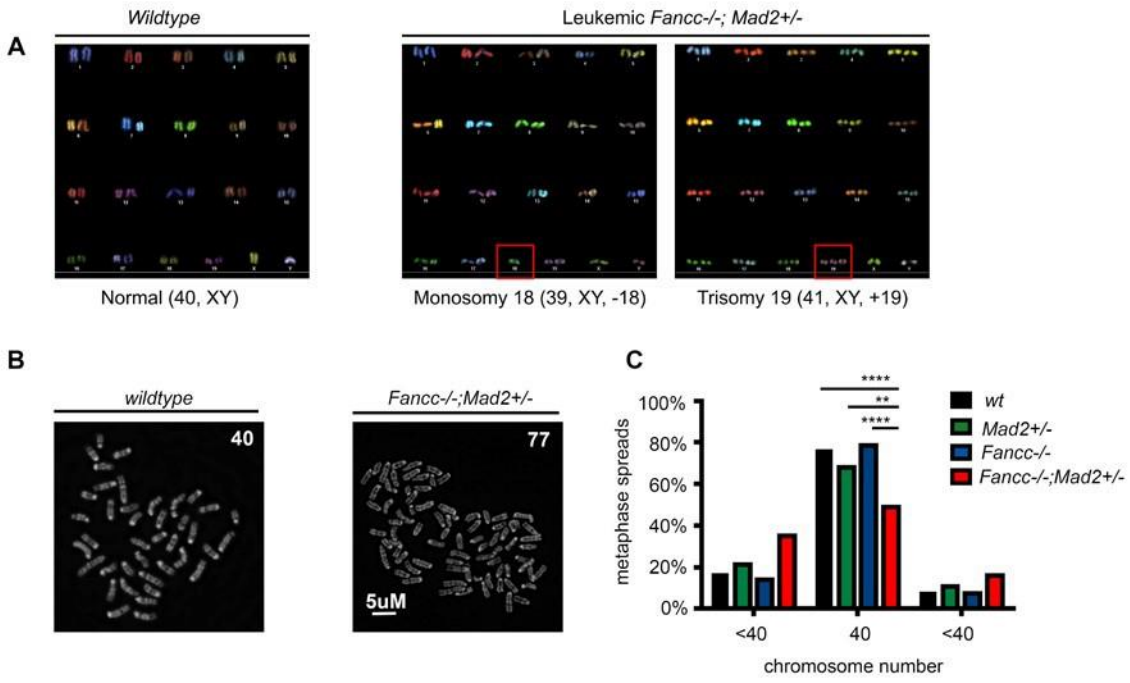

Figure 12. *Fancc-/-; Mad2+/-* hematopoietic cells are genomically unstable. (A) Representative images from spectral karyotyping of *wt* and leukemic *Fancc-/-;Mad2+/-* bone marrow cells. At least 11 cells/genotype were evaluated for cytogenetic abnormalities. (B) Example images of individual metaphase spreads made from bone marrow cells from age-matched healthy mice captured at 100x on a Deltavision deconvolution miscroscope. (C) Quantification of chromosome number per individual spread (n = 150 spreads/genotype), with statistical significance calculated by Fisher's exact test and Bonferroni post-hoc analysis. Murine cells have 40 chromosomes.

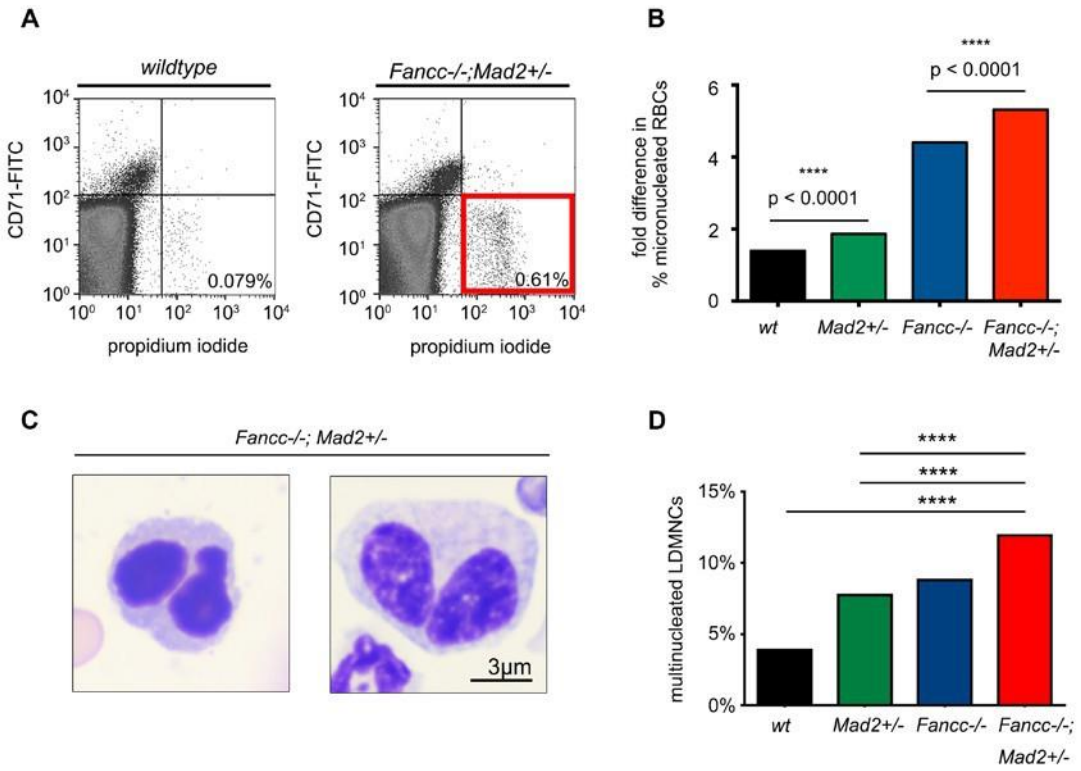

Figure 13. *Fancc-/-; Mad2+/-* hematopoietic cells display micronucleation and multinucleation. Flow profiles (A) from a red blood cell (RBC) micronucleation assay, identifying mature micronucleated RBCs as CD71-, propidium iodide+. Quantification of percentage of micronucleated cells in PB of mice shown as fold difference compared to controls (B). Data represents at least 9 age-matched animals/genotype with statistical analysis done via Fisher's exact test. (C) Representative images of multinucleated LDMNCs from healthy *Fancc-/-; Mad2+/-* mice and (D) quantification of percentage of multinucleated LDMNCs on Giesma-stained bone marrow cytospins. At least 800 cells/genotype were counted, and statistical significance was determined by Fisher's exact test. ***$p \leq 0.0001$, ** $p \leq 0.01$.

Heightened genomic instability in *Fancc-/-; Mad2+/-* animals is due to exacerbated SAC dysfunction

Finally, to demonstrate that the heightened genomic instability in the *Fancc-/-; Mad2+/-* mice was indeed due to exacerbated SAC impairment, we isolated ckit+ cells from the bone marrow of *Fancc-/-; Mad2+/-* and control mice, pulsed them with EdU and cultured them in the presence of 100ng/ml nocodazole for 12 hours. We then quantified the percentage of mitotic cells (EdU+, pHH3+ staining) and multinucleated cells (distinguished by nuclear morphology and EdU+, pHH3- staining) in each group. While the majority of *wt* ckit+ cells arrested in mitosis upon nocodazole treatment, the *Fancc-/-; Mad2+/-* cells failed to arrest and became multinucleated, demonstrating a heightened SAC impairment than that of both *Fancc-/-* or *Mad2+/-* groups with a single SAC gene deficiency (**Fig. 14A-C**). Phase-contrast live imaging of MEFs treated with 2μM taxol revealed a shorter time of mitotic arrest in the *Fancc-/-; Mad2+/-* genotype compared to *wt* and single mutant control cells (**Fig. 14D-E**), further demonstrating impaired SAC function in this genotype.

After determining the central role of SAC dysfunction in our model, and our knowledge that FA-associated genomic instability is driven by additional factors besides mitotic abnormalities, we next explored the DNA damage repair status of the *Fancc-/-; Mad2+/-* intercross. In methylcellulose progenitor assays with increasing doses of the crosslinking agent mitomycin C, *Fancc-/-; Mad2+/-* bone marrow progenitors demonstrated increased hypersensitivity to MMC similar to that of *Fancc-/-* mice (**Fig. 15A-B**). We also performed a chromosome breakage test by culturing LDMNCs of each genotype in 50nM

MMC for 48 hours, and then identifying chromosome breaks by microscopy of metaphase spreads. As expected, *Fancc-/-* cells displayed an increased frequency of breaks that was importantly not further exacerbated in the *Fancc-/-; Mad2+/-* cells (**Fig. 15C**). These studies eliminate the possibility of heightened DNA damage as a contributing factor to the increased aneuploidy and cancer predisposition of our intercrossed model.

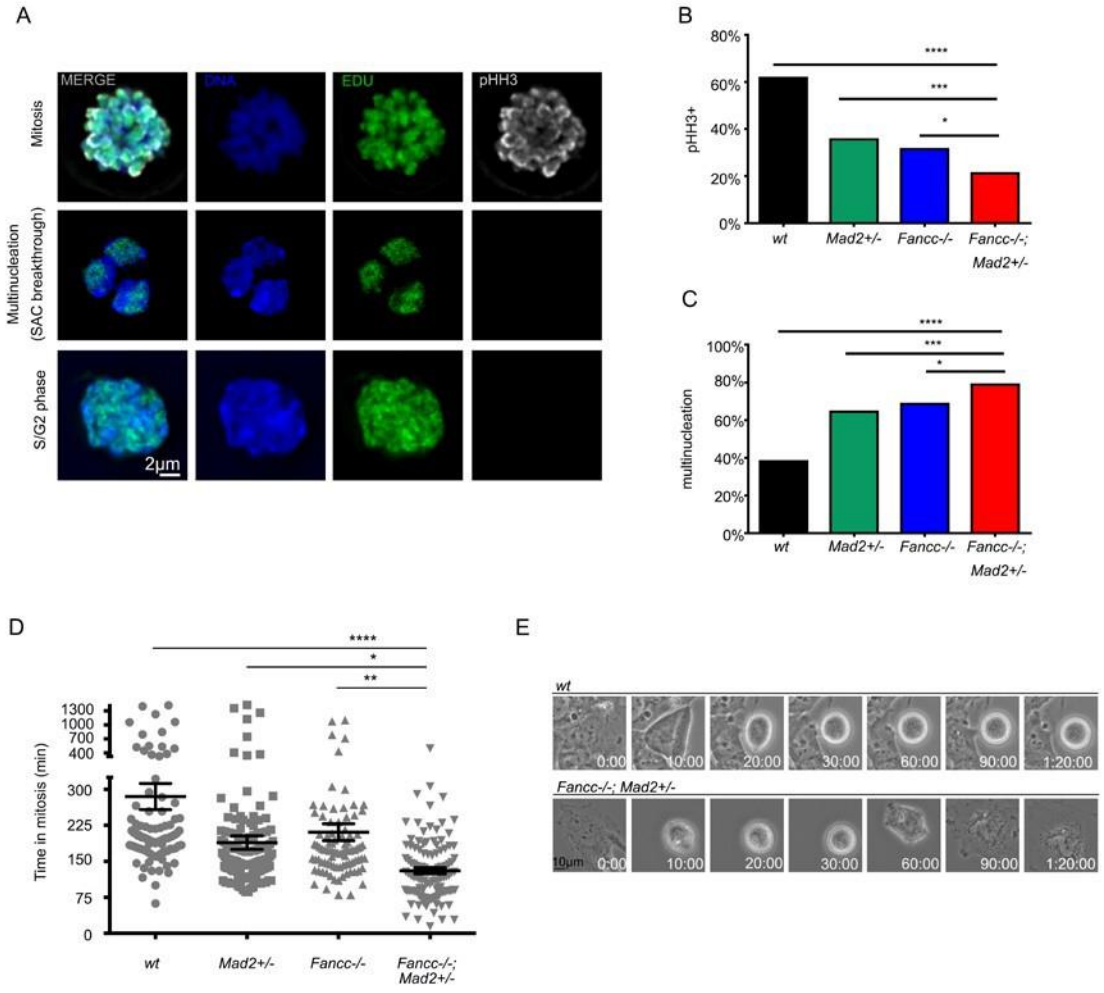

Figure 14. Genomic instability in *Fancc-/-; Mad2+/-* mice is due to exacerbated SAC dysfunction. (A) Example images of cell cycle phases observed in ckit+ bone marrow fraction after EdU pulse and incubation with 100ng/ml nocodazole for 12 hours. Percentage of mitotic cells (B) and multinucleated cells (C) per genotype were quantified. At least 200 cells/genotype were imaged, and Fisher's exact test was used for statistics. (D) Low passage mouse embryonic fibroblasts (MEFs) of each genotype were treated with 2μM taxol and imaged on a Nikon Biostation phase contrast live imaging microscope, which captured pictures at 2 minute intervals for 24 hours. Time in mitosis (defined as the onset of nuclear envelope breakdown until the time the nuclear envelope

reforms) was recorded for at least 90 cells/genotype, and analyzed by one-way ANOVA and Tukey's post-hoc multiple comparisons test. (E) Time lapse frames (minutes) demonstrating mitotic arrest of a *wt* cell in taxol (top panel) as compared with the SAC breakthrough and shortened mitosis of a *Fancc-/-; Mad2+/-* cell (bottom panel).

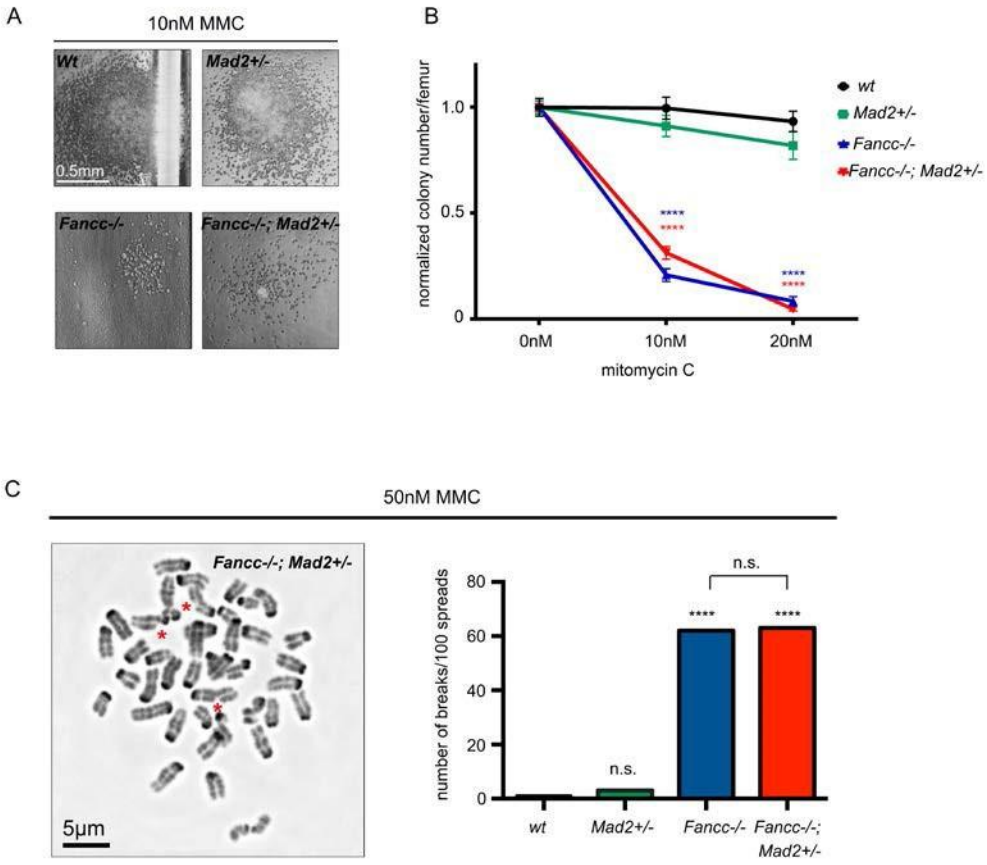

Figure 15. *Mad2* heterozygosity does not worsen the DNA damage repair (DDR) defect upon loss of *Fancc*. Hematopoietic colony forming assays were performed in varying doses of MMC, using LDMNCs from n =3 age-matched mice/genotype. (A) *Fancc-/-* and *Fancc-/-; Mad2+/-* progenitors formed smaller colonies in MMC and (B) fewer total colonies n a dose-dependent manner. Two-way ANOVA was performed, and statistics represent comparisons within genotypes compared to the control 0nM MMC treated group. (C) Chromosome breakage test was performed by preparing metaphase spreads from bone marrow cells treated with 50nM MMC for 48 hours. The number of breaks/cell (red asterisks) was quantified on the deconvolution scope, and demonstrate that both *Fancc-/-* and *Fancc-/-; Mad2+/-* cells have similar chromosome breakage

profiles in MMC. At least 100 cells/genotype were analyzed, and Fisher's exact test was used to determine significance. ****$p \leq 0.0001$.

DISCUSSION

We have generated a novel FA-SAC model via the intercross of *Fancc-/-* and *Mad2+/-* mice. *Fancc-/-;Mad2+/-* mice are predisposed to developing hematologic malignancies secondary to heightened aneuploidy and exacerbated SAC dysfunction. The majority of the malignancies seen in these mice are myeloid leukemia cases, faithfully recapitulating the common cancer seen in FA patients.

SAC impairment contributes to tumorigenesis in our mouse model, in which one of the core FA genes, *Fancc,* is deficient. There is also *in vivo* evidence that *Brca2*/*Fancd1*, regulates the SAC by promoting BubR1 acetylation in mitosis to protect genomic integrity (77, 78). Recently Vasanthakumar, et al generated a conditional *Brca1/Fancs* knock out mouse model that develops spontaneous BMF and displays cytogenetic abnormalities (61). Taken together, these models demonstrate the importance of FA signaling in regulating the SAC to prevent tumorigenesis.

Our model displays aneuploidy due to SAC dysfunction, and subsequent cancer predisposition. We know that aneuploidy can lead to tumorigenesis by unequal distribution of genetic material, potentially yielding a proliferative and evolutionary advantage to a daughter cell (50). Another mechanism by which aneuploidy can promote tumorigenesis is via chromothripsis, whereby one chromosome gets pulverized and undergoes massive structural rearrangements. This occurs when a micronucleus, formed from a missegregated lagging chromosome, undergoes DNA damage as it enters the

subsequent mitosis without having finished the previous replication (83). This catastrophic event can either compromise or heighten cell fitness. Identifying the micronucleus itself as a source of genomic instability in aneuploidy cells is a exciting concept that may be relevant to understanding genomic instability in FA, given that micronucleation and aneuploidy are hallmark FA features (84, 85). It is possible that this process is occurring in our FA-SAC model, an idea that will need further investigation.

Like our model, many other genetic models of aneuploidy display heightened cancer incidence (78, 86, 87). However, there are also mouse models of aneuploidy that are tumor suppressive (88, 89). Rationale behind this apparent contradiction is based on the difference of the rate of chromosome missegregation in different models. A lower rate of missegregation (one or two chromosomes per division) seems to promote cancer, while a CIN rate that exceeds a certain threshold (more than five chromosomes per division) rather leads to cell death and has a tumor suppressive effect (59, 88). Unsurprisingly then, complete loss of certain SAC genes, such as Mad2 and BubR1, are embryonic lethal (82). This dichotomy has sparked the idea of accelerating chromosome missegregation as a therapeutic strategy to target cancers with low rates of chromosome missegregation. For example, inhibition of CENP-E, a mitotic motor protein that controls chromosome alignment, in SAC-impaired cancer cells was shown to promote p53 activation and aneuploidy, which subsequently contributed to replication stress-mediated DSBs and proteotoxic stress (90). Given the FA pathway's central role in protecting genomic integrity by regulating the SAC, DNA damage repair, and genotoxic stress, utilization of such anti-mitotic therapies in FA-deficient tumors could be highly specific and effective

at halting tumor growth. Our FA-SAC model, which genetically induces chromosome missegregration that is tumor-promoting, may be a platform to test this strategy.

Our studies additionally demonstrate that deficiency of these two SAC regulators *Fancc* and *Mad2* cooperate to disrupt hematopoiesis. We observed MDS-post transplant and functional impairment in HSCs after transplant of *Fancc-/-; Mad2+/-* LDMNCs. In addition to its role at the SAC, Mad2 associates with c-kit, a tyrosine kinase receptor in immature hematopoietic cells, and *Mad2+/-* immature hematopoietic cells cycle less frequently than expected (91). Many additional SAC-associated proteins are known to be required for normal hematopoiesis, particularly in regulating the maturation of megakaryocytes. Interestingly, mature megakaryocytes become polyploid by the process of endomitosis, in which nuclear division occurs followed by failed cytokinesis (92). Heterozygosity of the mitotic checkpoint kinase *Bubr1* causes decreased pro-platelet forming ability of megakaryocytes (93). *Fanca-/-* mice have diminished platelet formation and decreased proliferation of megakaryocyte progenitors, demonstrating that *Fanca* is required for normal megakaryocyte differentiation (94). Also progression of the metaphase-to-anaphase transition relies on proteasome-dependent degradation, and pharmacologic inhibition of the proteasome blocks proplatelet formation (95). These studies, in concert with our observations in our FA-SAC model, support the importance of regulated SAC function in preserving normal hematopoiesis.

The current understanding of the pathogenesis of BMF and leukemia in FA relies on our understanding of how loss of FA signaling, the complex regulatory system protecting

genome integrity, affects the HSC. HSCs are a typically quiescent cell in the bone marrow, but when presented with physiological stress, can be provoked to exit their normal quiescent state. This exit from senescence provokes DNA-damage-induced attrition of the cycling HSCs, and subsequent p53 activation resulting in a BMF-like state (96), which given our findings, is likely in part due to compromised mitosis. Additionally, dividing HSCs that undergo erroneous mitosis increase the likelihood of clonal evolution, a phenomenon that has been seen in our model (**Fig. 11**) and after *ex-vivo* culture and transplant of *Fancc-/-* HSCs (97). Thus the impaired SAC mitotic function of FA-deficient cells likely cooperates with lack of DNA repair ability and an environment of genotoxic stress to create the perfect storm of disease progression.

Our findings highlight the tumor suppressive role of *Fancc* in maintaining the SAC to prevent aneuploidy and cancer development *in vivo*. We also know from our model that *Fancc* and *Mad2* act cooperatively to regulate the SAC. However, the signaling mechanism by which FANCC regulates the SAC during mitosis is still unclear. Kupfer et al has previously demonstrated that FANCC binds cyclin-dependent kinase 1 (CDK1), the mitotic checkpoint kinase whose activity must be silenced for mitotic exit (98). Additionally, FANCC is required for proper mitotic spindle formation and phosphorylation of stathmin-1, a regulator of microtubule dynamics (99). Interestingly, it was recently discovered that FANCC binds the E3 ubiquitin ligase Parkin (38), a protein that complexes with cdc20 to control mitotic progression (100). More work is needed to better understand the role of FANCC in the SAC and throughout mitosis.

FUTURE DIRECTIONS

We have characterized a novel FA-SAC whole-body transgenic model that develops hematopoietic-centered malignancies. Genetic disruption of *Mad2* and *Fancc* results in increased random aneuploidy and heightened risk for cancer. Although many of these mice spontaneously developed leukemias at a young age (<6 months), others did not succumb to malignancy until much later in life (18-24 months). We also did not observe any animals develop spontaneous BMF, though myelodysplasia was prevalent.

We would next like to pharmacologically challenge these FA-SAC animals to see if we can elicit a more robust phenotype in our model. We know that *Fancc-/-; Mad2+/-* hematopoietic cells are hypersensitive to taxol, and dosing these animals may elicit a BMF-like phenotype. On the other hand, we hypothesize that exposing the *Fancc-/-;Mad2+/-* animals to granulocyte colony stimulating factor (G-CSF), would increase the fraction of cycling hematopoietic cells, and given their impaired mitosis, accelerate the development of leukemias.

We are also expanding our genetic studies to include intercrossing *Fanca-/-* and *Mad2+/-* mice. We will compare the phenotype of these mice with our FA-SAC model to understand whether *Fanca* and *Fancc*, two core complex FA genes, act similarly to regulate the SAC.

Our ultimate goal with the FA-SAC model is to begin preclinical studies to probe the usefulness of antimitotic therapies for FA-related cancers. Direct treatment of leukemias

in *Fancc-/-; Mad2+/-* mice would likely be highly toxic, as these mice are whole-body transgenics. Instead we plan to transplant leukemia cells from *Fancc-/-; Mad2+/-* mice into irradiated congenic *wt* recipients, and then subsequently attempt to slow disease progression in recipients with antimitotic therapy such as taxol.

CHAPTER TWO

INTRODUCTION

Spindle assembly checkpoint signaling

The spindle assembly checkpoint senses the attachment state of kinetochores, and regulates the metaphase-to-anaphase transition to ensure proper chromosome segregation (101). The checkpoint inhibits the anaphase-promoting complex (APC/C), a mitotic ubiquitin ligase that facilitates the onset of anaphase. Upon binding to its activator CDC20, the APC/C promotes anaphase onset by degrading its substrates cyclin B1, the binding partner for the mitotic kinase cdk1, and securin, which blocks the protease separase to maintain sister chromatid cohesion (102). Upon sensing an unattached kinetochore, a hierarchy of SAC proteins is recruited to the kinetochore to activate the SAC, culminating in the recruitment of the proteins Mad1 and Mad2. Kinetochore recruitment of Mad2 prompts a change in its conformation from the free "open" conformation to its "closed" form (103). The closed conformation of Mad2 enables the formation of the mitotic checkpoint complex (MMC), consisting of the proteins Mad2, Bubr1, and Bub3 (104). The MCC sequesters CDC20, thus keeping the APC/C from being activated (104), and delaying anaphase onset until all kinetochores are properly attached to the mitotic spindle (**Fig. 16**).

The SAC can be activated through independent mechanisms of recruitment of Mad1/Mad2 to the KT (**Fig. 17**). When a KT is unattached to the spindle, Mad1/Mad2 KT recruitment occurs through two distinct signaling cascades, the KBB axis and the RZZ axis. Phosphorylation of the KT protein KNL1 recruits Bub1 and Bub3 (105),

forming the KBB complex that can recruit Mad1:Mad2. Additionally, unattached KTs recruit Zw10, Rod, and Zwilch—the RZZ complex—which also prompts Mad1:Mad2 localization to the KT (106, 107). The recent finding that unattached KTs can still recruit the RZZ and activate the SAC in the absence of KNL1 demonstrated that the KBB and RZZ axes independently recruit Mad1:Mad2 to the KT (108). Importantly, the strength of the SAC signal is based on the amount of Mad2 at the KT (109).

RZZ recruitment to the KT has been extensively studied. Stable KT localization of ZW10, a member of the RZZ complex, depends on its interaction with Zwint (110). This interaction requires Zwint phosphorylation by Aurora B kinase (111). Intriguingly, a pervious yeast two-hybrid screen identified Zwint as a potential interactor with Fancc, but did not validate the hit (112).

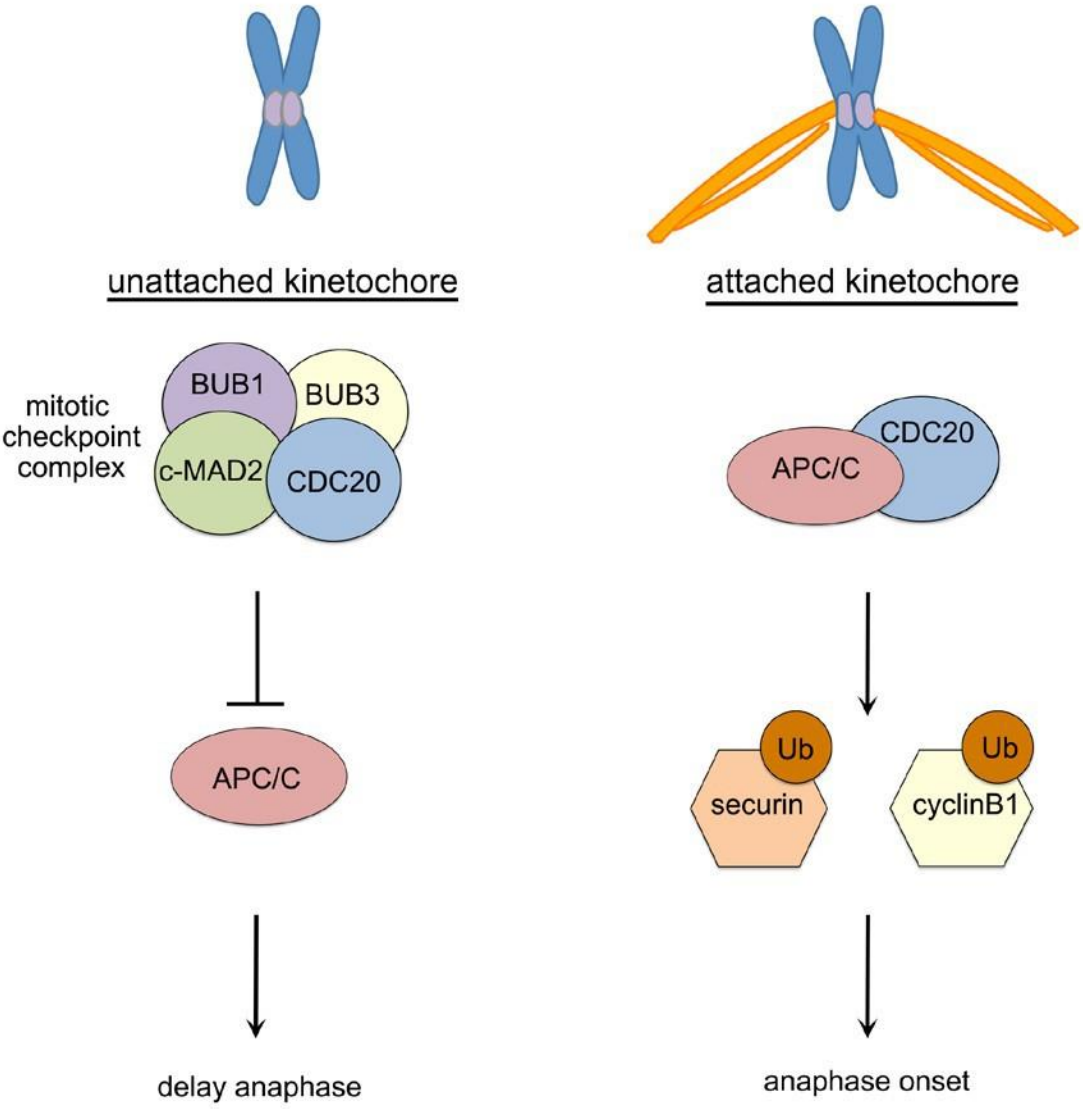

Figure 16. The SAC delays anaphase onset through MCC-mediated inhibition of the APC/C.

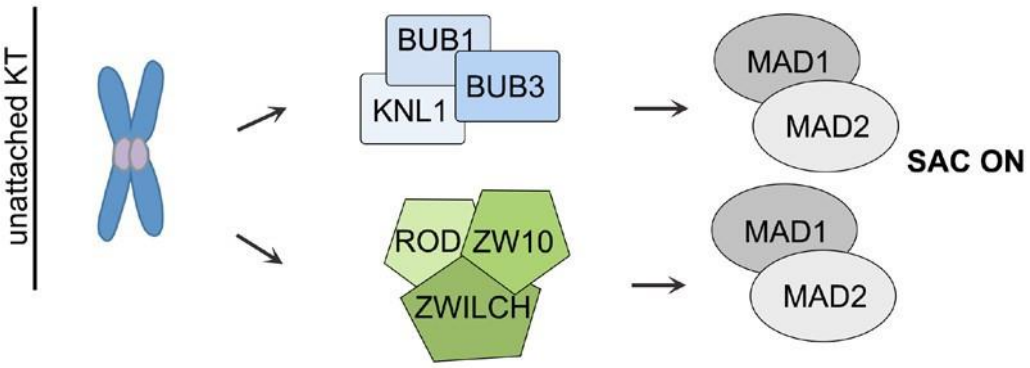

Figure 17. The KBB and RZZ pathways independently recruit Mad1/Mad2 to the KT to activate the SAC.

FANCC signaling at the SAC

Although it is well-established that FANCC regulates the SAC (43), little is known about the mechanism by which this occurs. Interestingly, Kupfer et al noted that FANCC binds CDK1 during the G2/M phase of the cell cycle (98), a finding that was highlighted years before any mitotic functions of FANCC were known. CDK1 is a mitotic kinase that is both a target and regulator of SAC response (101, 113). Thus we set out to further elucidate the CDK1-FANCC interaction at the SAC, and knowing the lack of epistasis between FANCC and MAD2 (see **CHAPTER ONE**), we hypothesized that FANCC signaling, though a possible interaction with Zwint, regulates the RZZ axis of the SAC.

MATERIALS AND METHODS

Cell culture

Patient fibroblast cell lines were cultured in DMEM supplemented with 15% FBS, 1% Penicillin-Streptomycin, 1% L-glutamine, and 1% Sodium pyruvate, and maintained in 37^{o}C, 5% O_2 incubators. HeLa cell lines were fed with 10% FBS and 1% Penicillin-Streptomycin in DMEM and cultured in 37^{o}C incubators.

Statistical analysis

Statistics were performed using Graph Pad Prism 6.0. Specific tests used and levels of significance are noted in the figure legends.

Immunofluorescence

Cells plated on coverslips were extracted for 30 seconds in 0.2% Triton diluted in PBS, and then fixed in 4% paraformaldehyde for 15 minutes at RT. Alternatively, for antibodies that did not need extraction, cells were directly fixed in 4% paraformaldehyde. Coverslips were then blocked in 0.2% Triton, 5% BSA solution in PBS for 1 hour. Coverslips were then incubated in primary antibody (diluted in PBS or 1% BSA-PBS, depending on antibody) overnight at 4^{o}C. Cells were washed three times with PBS, and then incubated in secondary antibody (Thermo Alexa 488 or 594 diluted 1:2000 in PBS or 1% BSA-PBS) at RT in the dark for 45 minutes. Cells were again washed in PBS, and mounted with ProLong Diamond Antifade mountant with Dapi (Thermo Fisher). Images were taken on a Deltavision deconvolution microscope, as described in CHAPTER ONE.

Primary antibodies

The following antibodies were used for western: anti-β-actin (Sigma); anti-FANCC (Santa Cruz, sc18110, 1:250); anti-Zwint (Abcam, ab168501, 1:1000); anti-FANCC (Abcam ab5065, 1:1000).

For immunofluorescence: anti-FANCC (ab97575, Abcam, 1:200); anti-CENPA (ab13939, Abcam 1:100); anti-Zwint (Abcam ab71982, 1:100); anti-Zwint (Abcam, ab168501, 1:100); anti-ZW10 (Abcam, ab21582, 1:100).

For immunoprecipitation: anti-FANCC (Santa Cruz, sc18110), anti-Zwint (Abcam ab71982).

Immunoblotting

Protein lysates were harvested using M-PER lysis buffer (Thermo Fisher) supplemented with protease inhibitor (Complete mini, Sigma) and phosphatase inhibitor cocktails (Pierce). Cell debris was pelleted for 5 minutes at 13,000rpm at 4^{o}C, and the supernatant saved for BCA protein quantification. After addition of SDS, lysates were boiled at 95^{o}C for 5 minutes, and loaded onto 4-12% Bis-Tris gradient gels (Thermo Fisher). Gels were run at 100-120V for 2 hours with MES running buffer. Proteins were then transferred onto nitrocellulose membrane. The membrane was blocked for one hour in Odyssey blocking buffer (Licor) and incubated in primary antibody diluted in blocking buffer overnight at 4^{o}C. After washing in PBS-T, the blot was incubated in fluorescent secondary antibody (Licor) diluted 1:5000 in blocking buffer for one hour in the dark, washed again with PBS-T, and developed using the Licor Odyssey CLx Imaging system.

Immunoprecipitation

For immunoprecipitation studies, 1mg protein was harvested from HeLa cells using MPER lysis buffer. The immunoprecipitation procedure was performed according to manufacturer instructions of the Thermo Fisher Crosslink IP Kit. Pulled-down protein eluted from the crosslinked column was denatured by SDS addition and developed by western blotting described above. Antibodies used for pulldown and western were derived from different host species.

Immunofluorescence quantification of kinetochore recruitment

Deconvolved image files were analyzed in Imaris software (version 7.7.1, Bitplane), using the spots function in surpass view mode. The region of interest was determined based on DAPI signal (DNA). The kinetochore signal (based on CENPA or ZWINT staining) was defined with xy diameter (0.3 μm) and ellipsoid size (0.6 μm) parameters. To eliminate background signal, the background subtraction Imaris function was used and a fluorescence quality threshold was set manually. The spots function then calculated the number of kinetochores with positive signal for the protein of interest and maximum intensity of signal per kinetochore. At least 300 kinetochores/group were used for analysis, and statistics were obtained using a student's t-test (for maximum intensity of signal at kinetochore) and a Fisher's exact test (for percentage of kinetochores with positive signal).

Pharmacologic inhibition of CDK1

For mitotic synchronization, HeLa cells were treated with 9μM R03306 (Sigma) for 22 hours, and then washed and released from G2 into mitosis for 30 minutes. After 30 minutes, 3 μM R03306 was added for an additional 30 minutes before harvesting cells. At this low dose, R03306 specifically inhibits CDK1, yet cells are still able to enter mitosis(114), so inhibition of CDK1 can be studied in a mitotic population. Cells were then stained with antibodies directed against either FANCC or ZW10 as described in above.

In vitro kinase assay

In vitro kinase assays were performed by incubating varying amounts of recombinant human FANCC protein (Abnova) with 1.25 U recombinant CDC2/cyclin B kinase (New England Biolabs) and 2ug histone H1 (CDC2 substrate) in kinase buffer (50 mM Tris-HCl, pH 7.5, 10 mM $MgCl_2$, 1 mM EGTA, 2 mM DTT, 40 mM β-glycerophosphate, 20 mM p-nitrophenylphosphate, 0.1 mM sodium vanadate, and 0.01% Brij 35) for 30 min in the presence of radioactive [P^{32}]γ-ATP (1 μCi). Reactions were terminated by running SDS-page and analyzed by autoradiography.

Protein phosphorylation site prediction

FANCC FASTA sequence was inputted into various online phosphorylation prediction sites: NetPhos2.0 (115), PhosphoNet (www.phosphonet.ca), and NetPhosK (116). Selected putative phosphorylation sites had a score > 0.90 (the closer to 1 indicates higher confidence of prediction), and were located within the known CDK1 binding region (98).

Plasmids & site-directed mutagenesis

C-terminal Myc-DDK-tagged FANCC cDNA in a PCMV6 entry vector was purchased from Origene. Site directed mutagenesis of FANCC was completed using the QuickChange XL site-directed mutagenesis kit (Agilent) and validated by Sanger sequencing. Mutagenesis and sequencing primers were generated using the NEBaseChanger website. Mutagenesis primers to generate S345A were: 5'-Cctactttccttacactgctccatctcttg-3' (forward) and 5'- Caagagatggagcagtgtaaggaaag-3' (reverse). Mutagenesis primers for S540A were: 5'- cgtcttggcattgaaggccctagatcag -3' (forward) and 5'- tttctgatctagggccttcaatgccaagac-3' (reverse). S543A was created using: 5- gcattgaaagccctagagcagaaaaac-3' (forward) and 5'- tcgggccagtttttctgctctagggctttc-3' (reverse). The following sequencing primers used were designed to cover the ORF of FANCC with overlapping reads: 5'-gtttagtgaaccgtcagaattttg-3'; 5'-gtaaacgaggccattttgc-3'; 5'-gctgggccacctcctggc-3'; 5-ctgagaggctgctgcttc-3'; 5'-gttcaggaaacagctatgaccg-3'; 5'-gccagaggcagactacag-3'.

Transfection

HeLa cells were transfected using the X-tremeGENE HP DNA transfection reagent (Roche) according to the manufacturer's protocol.

Virus generation & titration

To generate a virus backbone with desired neomycin selection, we cloned the SV40-Neo SV40-Neo^r/Kan^r-PolyA cassette from pCMV6-Entry-FANCC-DDK vector (Origene) to

pLenti-C-Myc-DDK vector (Origene). The SV40-Neo^r/Kan^r-PolyA cassette was cut out from pCMV6-Entry-FANCC-DDK vector by BspHI (NEB) digestion, and pLenti-C-Myc-DDK vector was linearized by XbaI (NEB) digestion. Both the SV40-Neo^r/Kan^r-PolyA fragment and the linearized pLenti-C-Myc-DDK backbone were blunted by DNA polymerase Klenow large fragment (NEB) and ligated by T4 DNA ligase (NEB). The presence and orientation of the SV40-Neo^r/Kan^r-PolyA fragment in the pLenti-C-Myc-DDK vector was confirmed by SfiI (NEB) digestion. We then cloned the FANCC (and mutant versions described above) from the pCMV6-backbone into the newly created pLenti-C-Myc-DDK-Neo^{r}Kan^r vector. The FANCC-DDK fragment was cut out from pCMV6-Entry-FANCC-DDK vector by SgfI and MluI digestion and inserted into pLenti-C-Myc-DDK-Neo^{r}Kan^r vector linearized by the same SgfI and MluI digestion. The final product is a lenti vector encoding FANCC-DDK and Neo^{r}Kan^r.

To generate virus, 293T cells (at 70% confluence) were transfected with 10ug of FANCC-DDK- Neo^{r}Kan^r –lentiviral vector (containing wildtype FANCC or site mutants), 5ug of helper plamis (pCD-NL/BH) and 1 ug foamyviral envelope containing plasmid (pcoPE01) in 6ml DMEM supplemented with 10% FBS and 0.0075mg/ml polyethyleneimine. After overnight incubation at 37^{o}C, media was replaced with DMEM supplemented with 10% FBS, 1% P/S, 1% glutamine, and 2% sodium bicarbonate, and incubated for an additional 24 hours. Virus was then concentrated by filtering through a polyethersulfone membrane (mesh size 0.45um) and centrifuging at 10,000rpm for 2 hours at 4 ^{o}C in 50ml conical tube. The viral pellet was resuspended in 1ml fresh DMEM, and utilized or stored in aliquots at -80^{o}C. Titration of the virus was determined by

seeding 50,000 HT1080 cells/ well of 6 well plate. Cells were serially transduced and percent GFP positivity via flow cytometry was used to calculate titer.

For transduction, virus was added to cell culture overnight, and media was replaced the next morning. 24 hours post-transduction, fibroblasts were selected with 0.4mg/ml G418 (Geneticin, Thermo fisher) for 5 days.

Sequencing of primary patient fibroblasts

Genomic DNA was isolated from primary cell pellet (BKBK cells) incubated in cell lysis buffer with Proteinase K at 56 ºC overnight. After addition of protein precipitation solution, the sample was centrifuged at 13000rpm for 10 min, and resuspended in cold isopropanol at -20 ºC for 20 minutes. The precipitated DNA was then washed with 70% ethanol, and resuspended in water. Multiple primer sets (forward and reverse) were designed using SnapGene version 3.3 to flank each of the 14 exons of *FANCC*. Primers were used for both amplification of the exon from genomic DNA as well as Sanger sequencing. Primer sequences used were as follows:

exon	Primer set (written 5' to 3')
1	F: gacttctagcctaatgatagtatcatg R: gtgtcatgtaacaatacagc
2	F: gcctttactgactattaagtatgagtag R: gtagatatttaaatcatctgggag
3	F: gaccacacaagagttaagtg

	R: ggaattcacagtcaagc
4	F: catgtacaaataaattgtaggcattg R: gttaaacatctcttctggaggactg
5	F: gacctgtctattgttcattgc R: ctcaccaatttgctatgtattccac
6	F: gacactgaaacagcaatggtag R: gctgtcgtacagtctttccaac
7	F: cttccatcactagacatttgcttattc R: gcatgctccaaggatg
8	F: caggcacacttcagtagaac R: gcctaactcaattctgtgtttc
9	F: gtacagagtatgcaagcctg R: catgacagagttctcagac
10	F: gtgaagtagaactcataaagacatc R: gtgatcacaactgggaag
11	F: gatgttcaactctgtgtgacatggac R : gatggtcccagaccag
12	F: cagtgcctgtcctcactg R: gcctgcaggttgccatgac
13	F: gactacattctgttgagaac R: ctgcgatggaaagaaatgtacg
14	F: gtccctggacaaaggacaaatc R: gctcattctcacagcccag

Patient fibroblast time-lapse imaging

Cells were plated into High-Q4 culture dishes (Nikon) for live imaging, and treated with 2.5mM thymidine for 16 hours for synchronization. Cells were then washed and released into 15% FBS in DMEM and placed on a Biostation IMQ live imaging microscope equipped with a 37^{o}C incubator. Phase contrast images (distance between z sections: 2µm) were captured at 2-minute intervals for 24 hours. Analysis was done using Nikon NIS-Elements Viewer software.

Patient fibroblast colony forming assays

For colony assays, 500 cells/10-cm dish were plated in 4 replicates. Cells were cultured for 11 days with varying doses of MMC and then plates were washed with 1x PBS and stained with methylene blue to highlight colonies.

Patient fibroblast cell cycle assays

To evaluate fibroblast cell cycle profiles after MMC treatment, patient fibroblasts were treated with 120nM of MMC for 2 hours, then washed and released into growth media for 24 hours. Cells were then harvested using HyQTase Cell Detachment reagent (GE Life Sciences), washed with PBS, and fixed in 70% ethanol at -20^{o}C overnight. Cells were then pelleted, washed with PBS, and stained with FxCycle PI/RNase Staining Solution (Life Technologies). At least 10,000 events were acquired on a BD FacsCanto Flow cytometer, and cell cycle profiles were obtained using FlowJo software.

To analyze SAC function of fibroblasts, transduced cells were plated onto coverslips and treated with 200nM taxol for 22 hours. Coverslips were fixed in 4% paraformaldehyde for 15 minutes, and then stained for alpha tubulin (1:100) and mounted in pro-long diamond antifade mountant with DAPI as described in Chapter one. Cells were visualized at 60x on a Deltavision deconvolution microscope, and the percentage of mitotic versus multinucleated cells was determined. At least 200 cells/experimental group were counted, and statistics was performed using Fisher's exact test.

RESULTS

CDK1 phosphorylates FANCC to localize FANCC to the mitotic spindle

CDK1 was identified as a binding partner of FANCC nearly two decades ago (98) before the mitotic functions of FANCC were discovered. Given the importance of CDK1 kinase activity in regulating mitotic exit (101), we hypothesized that FANCC is a target for CDK1 phosphorylation. To test this hypothesis, we performed an *in vitro* kinase assay, in which recombinant cdk1 (cdc2-cyclin B1) was incubated with increasing amounts of recombinant FANCC in the presence of radioactive [P^{32}] γ-ATP. Indeed, we detected phosphorylation of FANCC *in vitro* (**Fig. 18**) by CDK1. Interestingly, the ability of CDK1 to phosphorylate the general substrate histone H1 did not change with increasing doses of FANCC, indicating that the presence of FANCC does not alter CDK1 kinase activity *in vitro*.

CDK1 phosphorylates numerous substrates during mitosis to regulate substrate localization and function. To explore whether CDK1 activity is required for FANCC localization at the mitotic spindle, we treated HeLa cells with a low dose of the CDK1-specific inhibitor RO-3306 and observed FANCC localization by immunofluorescence. Interestingly, FANCC localization to the mitotic spindle in metaphase cells was lost in the presence of RO-3306 (**Fig. 19A**). Western blotting of FANCC expression showed no difference in total protein levels between untreated and RO-3306-treated samples (**Fig. 19B**).

Next, we used phosphorylation site prediction software to predict what residue(s) on FANCC may be phosphorylated by CDK1. We identified two hits, serine 540 and serine 543, (**Fig. 20**) that were predicted through multiple independent queries (NetPhos 2.0, PhosphoNet, and NetPhosK software). These residues had prediction scores > 0.9, and are located in the C-terminus of FANCC, the region of FANCC known to bind CDK1. Using a FANCC-DDK tagged pCMV6 plasmid, we performed site directed mutagenesis to generate S543A and S540A DDK-tagged phospho-dead mutant constructs. We then stably transfected the DDK-tagged FANCC mutants, along with wildtype FANCC-DDK into HeLa cells. Using an anti-DDK antibody to visualize localization of the tagged FANCC proteins during mitosis, we observed spindle localization of FANCC-DDK and S540A-DDK proteins (**Fig. 21**). However, S543A-DDK failed to localize to the spindle (**Fig. 21**), identifying serine 543 on FANCC as the site for CDK1 phosphorylation.

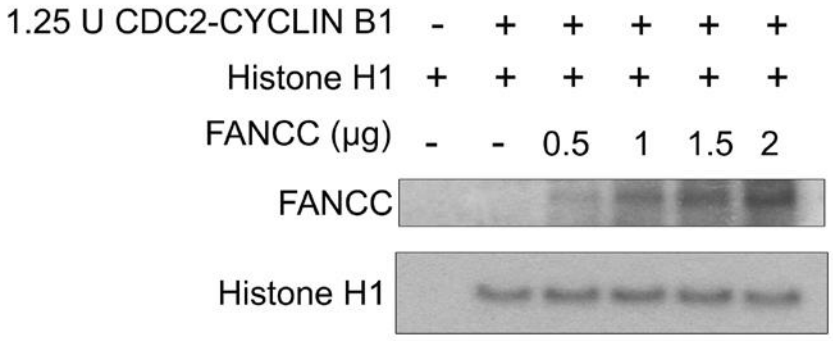

Figure 18. CDK1 phosphorylates FANCC in vitro. In vitro kinase assay demonstrates dose-dependent phosphorylation of recombinant FANCC by cdc2-cyclin B1 in the presence of radioactive ATP.

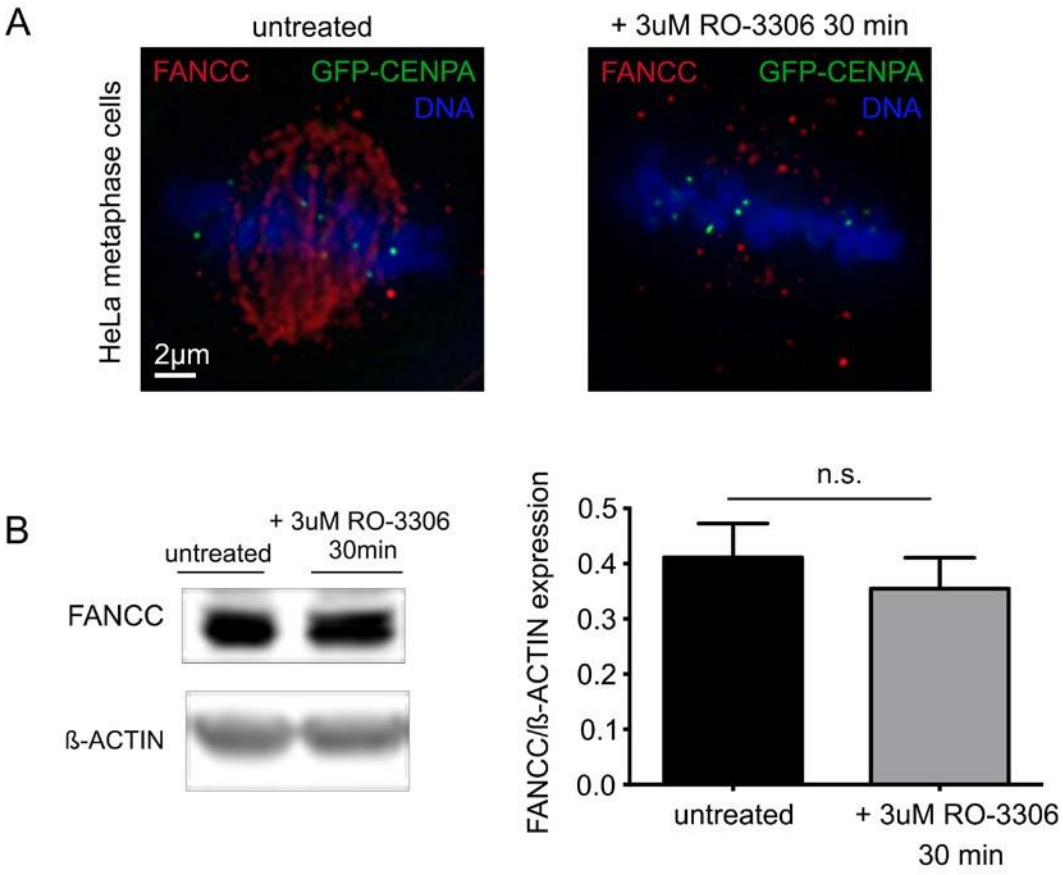

Figure 19. Pharmacologic CDK1 inhibition disrupts FANCC localization to the mitotic spindle. (A) FANCC (red) localization to the mitotic spindle (right) is lost upon treatment with CDK1-inhibitor RO-3306 (left). Images represent slices (200nm) taken at 100x on a Deltavision deconvolution microscope and deconvolved using Softworx software. Fancc protein expression in HeLa lysates was not affected by CDK1 inhibition (B, C). Quantification was performed using a Licor (Odyssey) CLx imaging system (n = 6 recplicates/treatment group), and a student's t-test was used to determine significance. Error bars represent SD.

Figure 20. Predicted CDK1-phosphorylation sites on FANCC. Putative phosphorylation sites (asterisk) were predicted using NetPhos 2.0, PhosphoNet, and NetPhosK sites, and had a prediction score > 0.90.

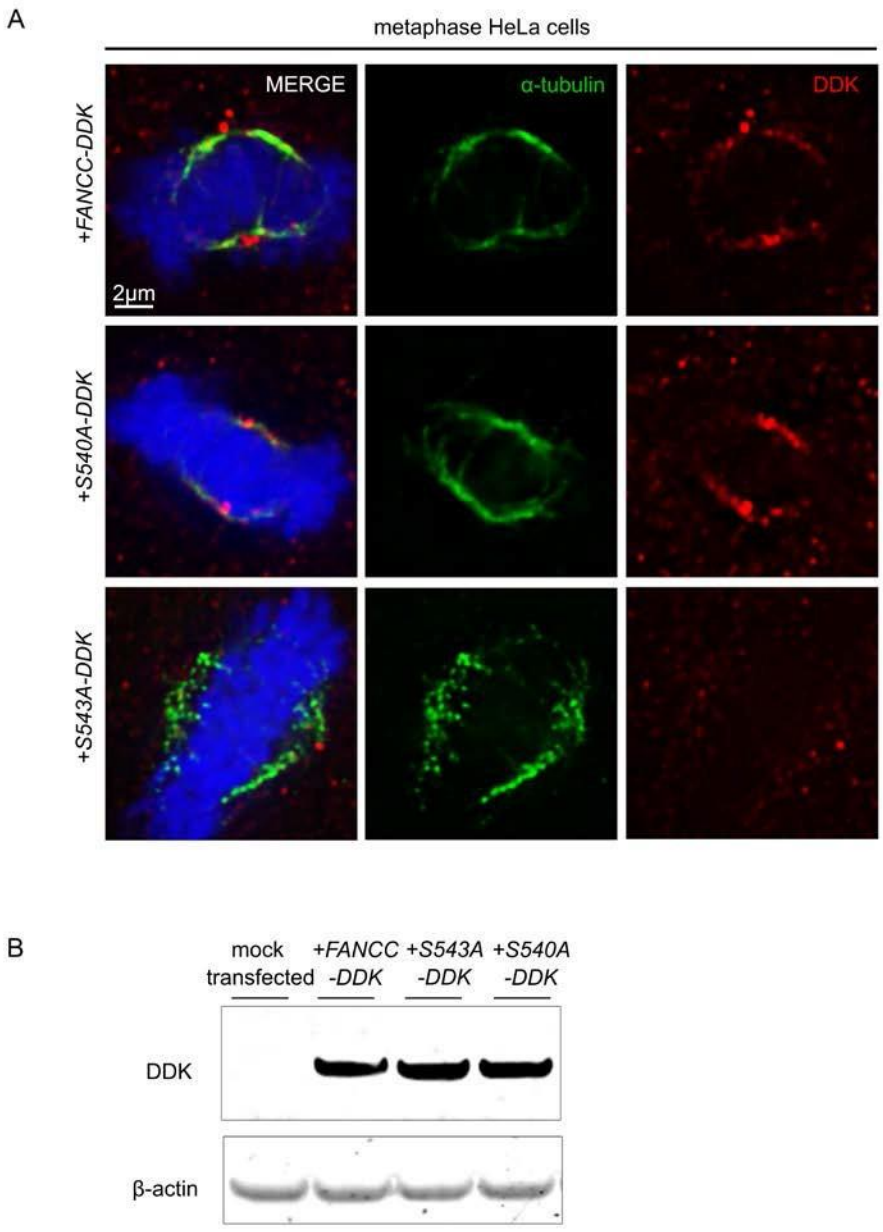

Figure 21. Phosphorylation at S543 is required for mitotic localization of FANCC. (A) HeLa cells transfected with *FANCC-DDK*, *S540A-DDK*, or *S543A-DDK* were stained with anti-alpha tubulin (green) to mark the mitotic spindle and anti-DDK (red). Images represent one slice (distance between z sections: 0.2μm) of an image stack from the deconvolution microscope (100x magnification). (B) Western of DDK expression in HeLas post-transfection.

FANCC SAC function requires CDK1-dependent phosphorylation

To explore whether phosphorylation at site 543 is important for FANCC mitotic function, we subcloned the genes encoding the FANCC-DDK and mutants into lenti-vectors and transduced a *FANCC*-deficient patient fibroblast primary cell line termed *BKBK* with the constructs. We sequenced DNA isolated from *BKBK* cells, and identified a bilallelic two base pair deletion (c.377_378del) in Exon 4 causing a frame shift (**Fig. 22**). After transduction and selection, we confirmed expression of our constructs by western blotting for both FANCC and DDK expression (**Fig. 23**).

To test whether phosphorylation of site 543 on FANCC was essential for the ability of FANCC to regulate the SAC, we quantified the time from NEB to anaphase onset via time lapse imaging of *BKBK-empty-DDK, BKBK-FANCC-DDK, and BKBK-S543A-DDK* fibroblasts. *BKBK-FANCC-DDK* cells demonstrated a longer duration of NEB to anaphase onset than either *BKBK-empty-DDK* or *BKBK-S543A-DDK* cells (**Fig. 24A**). Faster time through mitosis is suggestive of impaired SAC function. SAC function in these cells was also directly challenged by exposure to 200nM taxol and subsequent immunofluorescence to identify mitotic arrested cells versus multinucleated cells that had broken through arrest. While addition of FANCC-DDK to the BKBK cells rescued the SAC breakthrough of BKB-empty cells, addition of S543A-DDK failed to rescue the multinucleation phenotype seen in taxol (**Fig. 24B**). Taken together, these experiments suggest that phosphorylation of site 543 is crucial to the SAC function of FANCC.

Given FANCC's essential role in protecting genomic instability during both interphase and mitosis, we asked whether the S543A mutation would disrupt FANCC's interphase DNA repair function. Upon exposure to the DNA crosslinker mitomycin C (MMC), *S543A-DDK* cells fail to rescue the G2-arrest seen in *BKBK-empty-DDK* patient fibroblasts (**Fig. 25A**). Additionally, *BKBK* cells transduced with *S543A-DDK* maintain hypersensitivity to MMC in colony forming assays (**Fig. 25B**), a hallmark feature of FA. Interestingly, phosphorylation of S543 is also necessary to preserve the DDR function of FANCC.

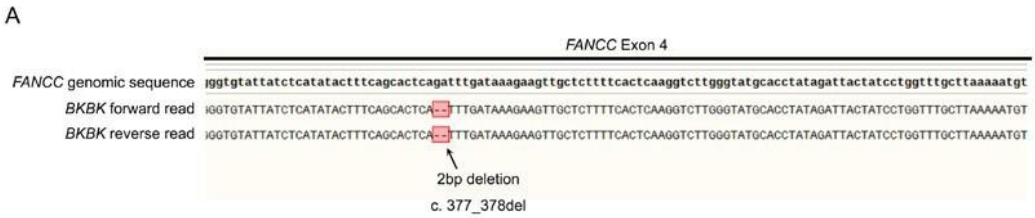

Figure 22. Sanger sequencing of *FANCC* patient fibroblast primary cell line *BKBK*. SnapGene software was used to align sequence with reference genomic *FANCC* sequence. The cell line was found to have bilallelic mutation c.377_378del in Exon 4, causing a frame shift and likely a truncated protein.

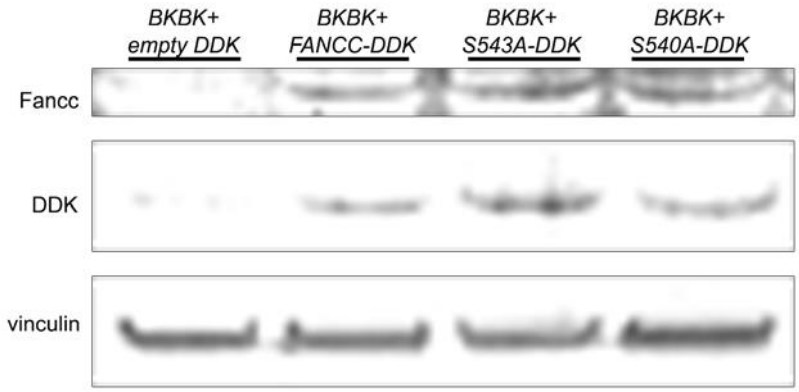

Figure 23. Confirmation of construct expression by western in *FANCC*-deficient *BKBK* patient fibroblasts after transduction and selection.

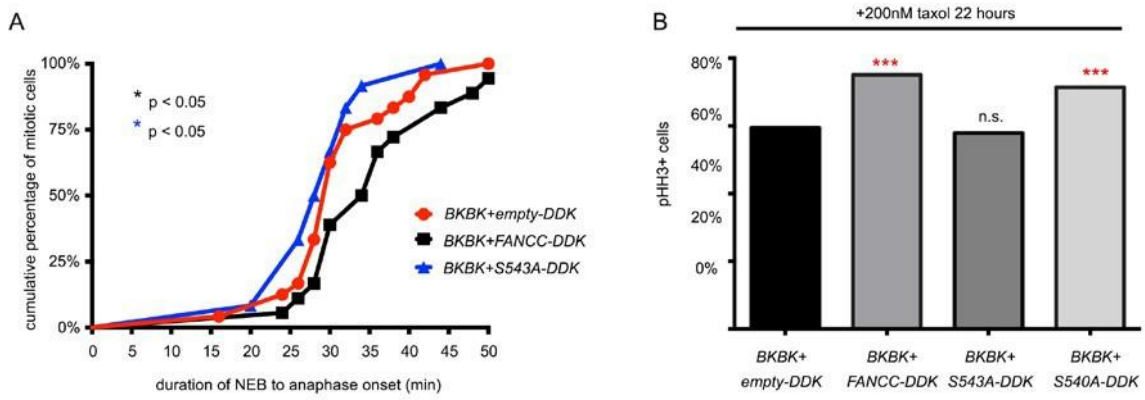

Figure 24. CDK1-dependent phosphorylation of S543A is required for FANCC SAC function. (A) Quantification of timing from nuclear envelope breakdown (NEB) to anaphase onset in mitotic *BKBK* cells transduced with *empty-DDK*, *FANCC-DDK*, or *S543A-DDK*. Time-lapsed phase contrast movies were acquired on a Nikon Biostation live imaging scope, and statistics represent comparisons to *BKBK+empty-DDK* via one-way ANOVA with Dunnet's multiple comparisons test. (B) SAC challenge of *BKBK* cells transduced with *empty-DDK*, *FANCC-DDK*, *S543A-DDK*, or *S540A-DDK*. The percentage of pHH3+ cells was quantified, and significance determined using Fisher's exact test. Significance is shown compared to *BKBK+empty-DDK*; *** $p < 0.001$ with $p < 0.017$ considered significant to account for multiple comparisons.

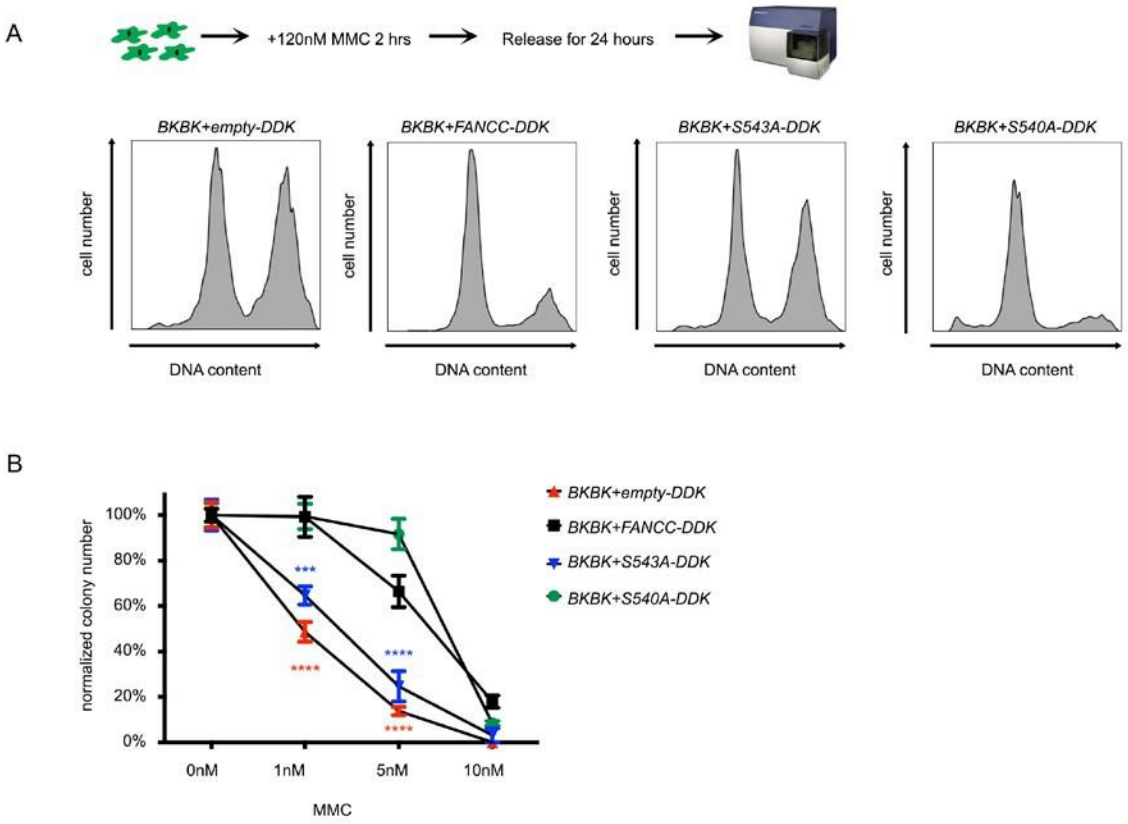

Figure 25. Phosphorylation of FANCC at S543 is necessary for FANCC interphase DDR function. (A) After exposure to MMC, *S543A-DDK* cells fail to rescue the G2-arrest seen in *BKBK-empty-DDK* patient fibroblasts. (B) *BKBK* cells transduced with *S543A-DDK* maintain hypersensitivity to MMC, a hallmark feature of FA. Statistical significance was determined by two-way ANOVA, and p values represent comparisons with *BKBK-FANCC-DDK*, *** $p < 0.001$, **** $p < 0.0001$.

FANCC interacts with the kinetochore protein ZWINT

Although we identified CDK1 phosphorylation as important for FANCC SAC function, the signaling mechanism by which phospho-FANCC regulates the SAC is still unclear. Another research group previously performed a yeast-two hybrid screen to identify interactors of FANCC (117), and the kinetochore protein ZWINT was listed as an unvalidated hit from the screen. Given ZWINT's importance in binding ZW10 to ensure stable ZW10 kinetochore localization (110), an important step in RZZ recruitment and SAC activation, we confirmed this interaction biochemically in HeLa cells. Indeed, co-immunoprecipitation experiments demonstrated that FANCC and ZWINT are together in a protein complex (**Fig. 26**).

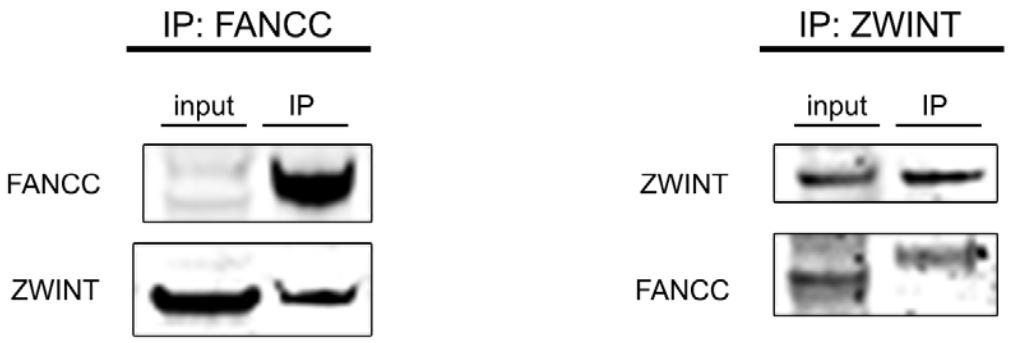

Figure 26. FANCC interacts with the kinetochore protein ZWINT.

Immunoprecipitation of FANCC (left) and blotting for ZWINT, and pulldown of ZWINT (right) and blotting for FANCC in HeLa lysates demonstrate FANCC-ZWINT binding.

Loss of FANCC impairs stable localization of ZW10 at prometaphase kinetochores

Because FANCC regulates the SAC, and ZWINT is recruited to unattached KTs to activate downstream SAC effectors, we explored whether FANCC is required to recruit Zwint to the KT. Using our *FANCC*-deficient patient fibroblast line and an isogenic *FANCC*-corrected line as a control, we did immunofluorescence imaging of ZWINT in prometaphase cells. Although FANCC and ZWINT are binding partners, loss of FANCC did not impact ZWINT KT recruitment (**Fig. 27**). ZWINT is known to recruit ZW10, a member of the RZZ complex, to the KT to facilitate the SAC response. Interestingly, we observed disrupted ZW10 KT localization in *FANCC*-deficient fibroblasts (**Fig. 28**), suggesting that FANCC-ZWINT binding may be required for ZW10 recruitment and SAC activation at the KT. ZW10, as a member of the RZZ complex, is known to recruit the SAC effector MAD2 to the kinetochore, and so we asked whether loss of FANCC would disrupt MAD2 kinetochore localization. Indeed, we observed decreased MAD2 recruitment to prometaphase KTs in *FANCC*-deficient patient fibroblasts (**Fig. 29**).

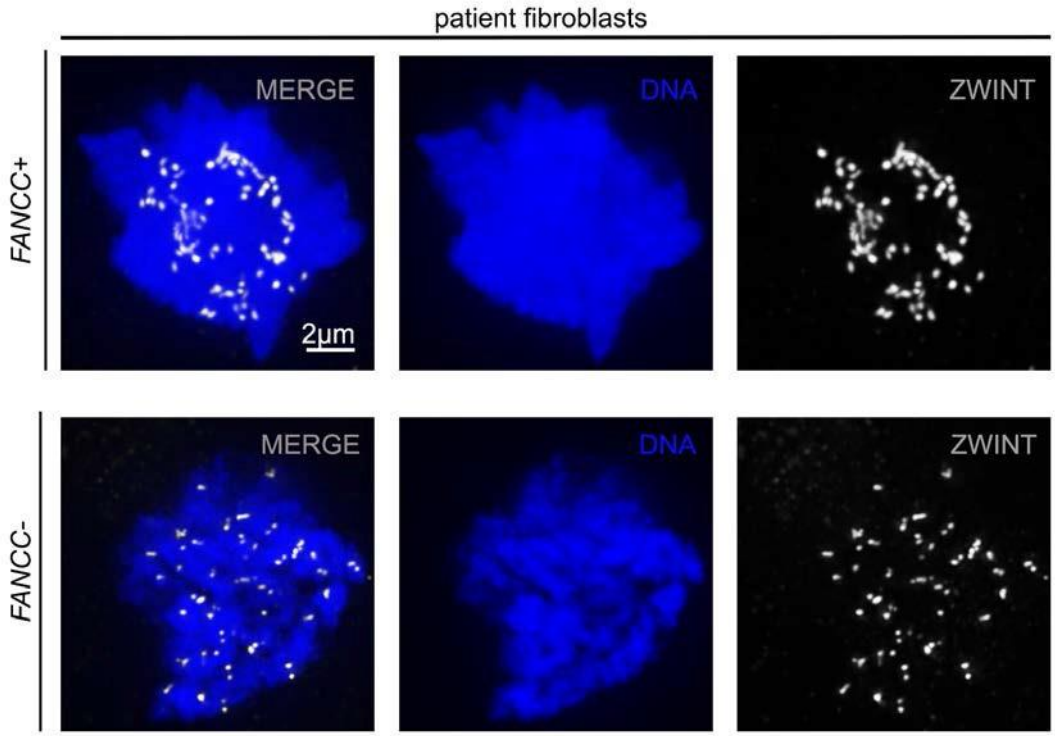

Figure 27. Loss of FANCC does not disrupt ZWINT kinetochore localization during prometaphase. Representative images *FANCC* corrected and uncorrected patient fibroblasts stained with anti-Zwint antibody (white) and DAPI to highlight DNA.

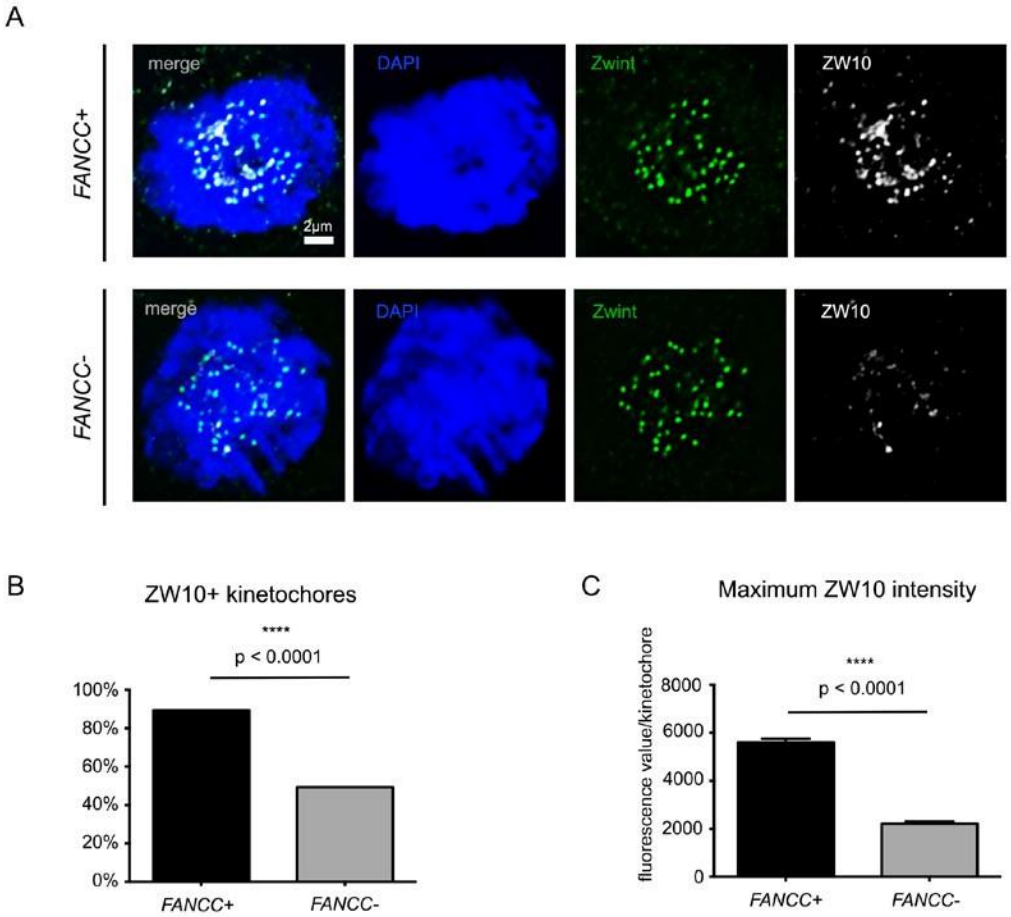

Figure 28. Loss of FANCC impairs stable localization of ZW10 at prometaphase kinetochores. (A) Representative images of ZW10 (white) localization to kinetochore (marked by Zwint stain, green) during prometaphase in *FANCC*-deficient and *FANCC*-corrected fibroblasts. Quantification in Imaris depicts less ZW10+ kinetochores (B) and decreased maximum ZW10 fluorescence intensity at the kinetochore (C) in *FANCC*-deficient patient fibroblasts. At least 500 kinetochores/group were analyzed, and statistics were obtained via student's t-test.

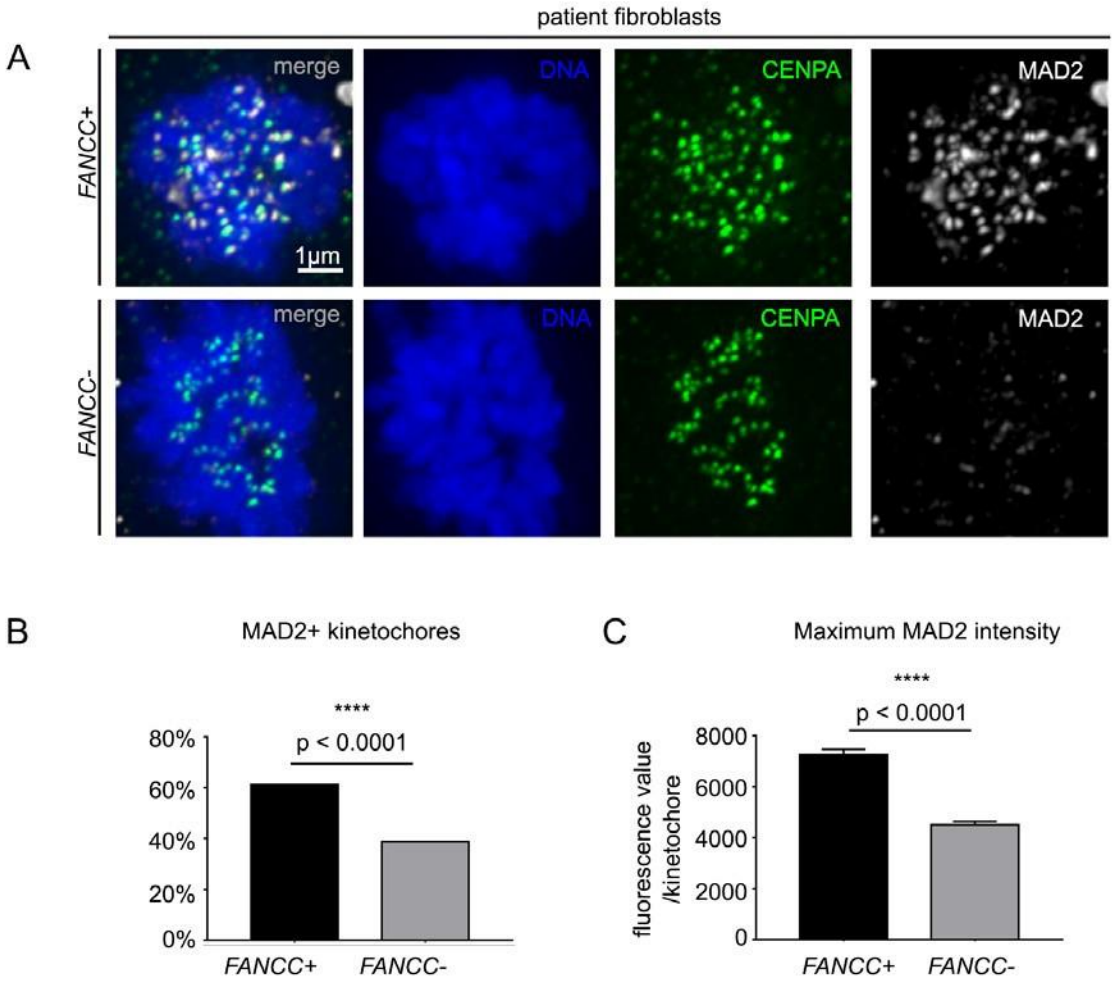

Figure 29. Loss of FANCC impairs MAD2 localization to the prometaphase kinetochore. (A) Representative images of MAD2 (white) localization to the CENPA+ kinetochores (green) in *FANCC*-corrected and uncorrected patient fibroblasts. Quantification demonstrates decreased percentage of kinetochores with MAD2 positivity (B) and decreased fluorescence signal intensity of MAD2 at kinetochores (C) in *FANCC*-deficient cells. At least 300 kinetochores/cell line were analyzed using Imaris software, and statistical significance was established using Fisher's exact test (B) and student's t-test (C).

CDK1-dependent phosphorylation of FANCC is necessary to recruit ZW10 to the prometaphase kinetochore

Having established the importance of CDK1 phosphorylation for FANCC function, we asked whether this phosphorylation event is necessary for FANCC's ability to recruit ZW10 to the KT. Interestingly, pharmacologic inhibition of CDK1 in HeLa cells disrupted ZW10 localization to the kinetochore during prometaphase (**Fig. 30A-C**), while ZW10 total protein expression was unaffected (**Fig. 30D-E**). More specifically, ZW10 expression at the KT was decreased in *BKBK* cells expressing the phospho-dead *S543A-DDK* compared to *BKBK-FANCC-DDK* cells (**Fig. 31**). Thus phosphorylation of FANCC at S543 by CDK1 regulates the SAC by facilitating ZW10 recruitment to the KT.

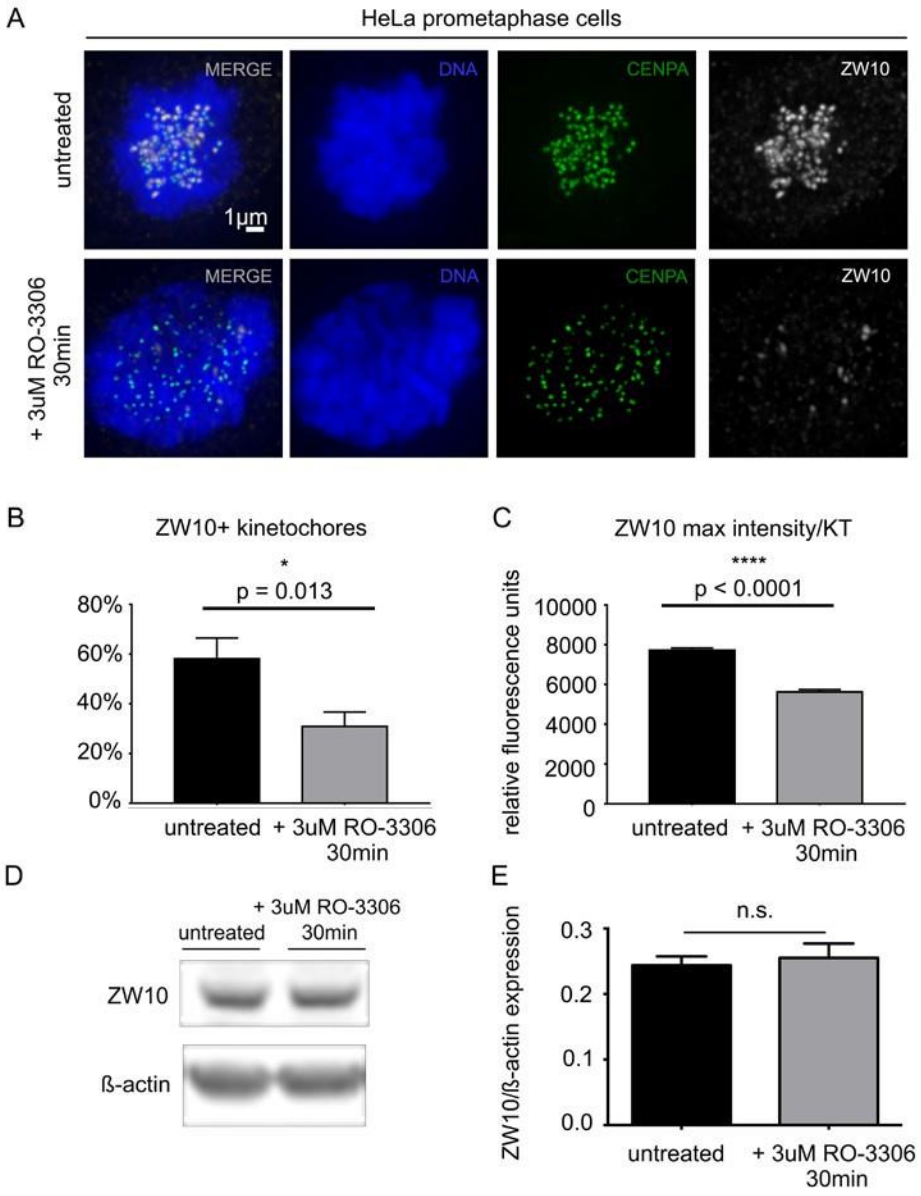

Figure 30. Pharmacologic inhibition of CDK1 during mitosis disrupts ZW10 kinetochore recruitment. (A) Immunofluorescence images of ZW10 localization (white) in untreated and RO-3306 –treated HeLa cells in prometaphase. CENPA (green) was used as a kinetochore marker, and DNA is shown in blue. Quantification demonstrates less ZW10+ kinetochores (B) and decreased ZW10 kinetochore fluorescence intensity (C) upon CDK1 inhibition. At least 2000 kinetochores were quantified using Imaris Bitplane software. Total protein expression of ZW10 in HeLa

lysates was not affected by CDK1 inhibition (D, E). Quantification (E) was performed using Licor Odyssey software and represents at least 6 replicates. Error bars represent SEM, with student's t-test used for statistics.

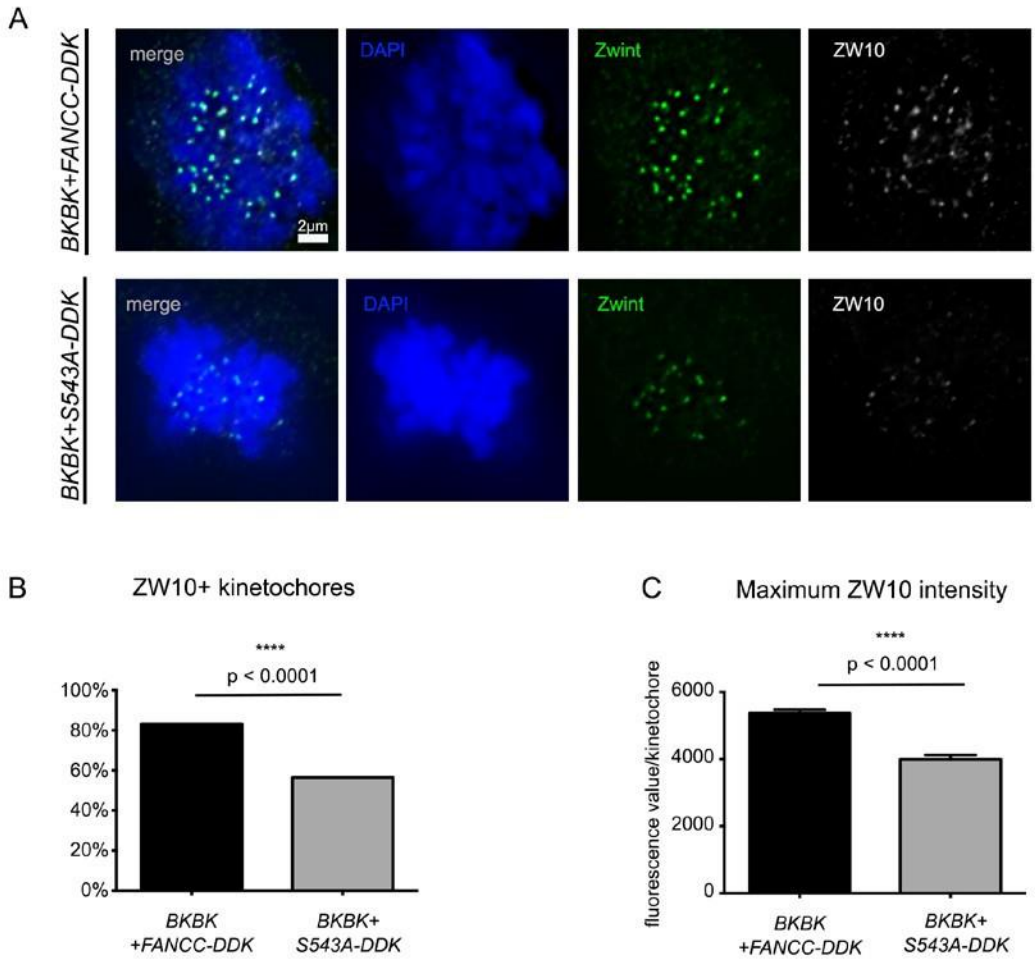

Figure 31. Phosphorylation of FANCC at S543 is necessary for stable ZW10 kinetochore recruitment. (A) Representative images of *FANCC-deficient BKBK* prometaphase fibroblasts expressing either *FANCC-DDK* or *S543A-DDK.* DNA is shown in blue, and cells were stained with anti-ZWINT (green) and anti-ZW10 (white) antibodies. Quantification shows less ZW10+ kinetochores (B) and decreased maximum ZW10 fluorescence intensity at kinetochores (C) in *BKBK-S543A-DDK* cells. Image analysis was performed using Imaris Bitplane software, with at least 500 kinetochores analyzed per group. Statistical significance was determined using student's t-test.

DISCUSSION

We have elucidated a novel CDK1-FANCC-ZW10 signaling axis (**Fig. 32**) that provides a mechanism by which FANCC regulates the SAC to prevent aneuploidy and genomic instability. We now know that CDK1 phosphorylates FANCC at serine 543, and that this phosphorylation event is necessary for the mitotic localization of FANCC and its SAC function. We have also demonstrated that phosphorylation at S543 is needed for the KT recruitment of ZW10, which promotes the recruitment of Mad1/Mad2 to activate the SAC.

FANCC-RZZ signaling

We have shown that phosphorylation of FANCC is required for ZW10 kinetochore recruitment. ZW10 is a member of the RZZ complex, consisting of ROD, ZWILCH and ZW10. ZW10 is required for the recruitment of ROD to the KT, and vice versa (118). We hypothesize that loss of FANCC disrupts KT localization of the RZZ complex as a whole, in addition to ZW10, and are currently examining KT recruitment of ROD and ZWILCH in *FANCC*-deficient cells.

While we demonstrate that FANCC is necessary for ZW10 KT recruitment, the process by which this occurs is still unclear. We have shown that FANCC binds Zwint during prometaphase, but have been unable to co-immunoprecipitate ZW10 and FANCC (data not shown), suggesting that FANCC indirectly recruits ZW10. Loss of FANCC results in impaired recruitment of ZW-10, but not Zwint, to KTs. Zwint must be phosphorylated by

Aurora kinase B in order to interact with ZW-10 and facilitate ZW-10 recruitment to the KT. Pharmacologic inhibition of Aurora kinase B activity results in impaired recruitment of ZW-10, but not Zwint, to the KT (111). Based on the phenotypic similarities between loss of FANCC and inhibition of Aurora kinase B (**Table 3**), we hypothesize that FANCC may facilitate Aurora kinase B-mediated phosphorylation of Zwint to ensure KT recruitment of the RZZ complex and SAC activation.

The RZZ complex, in addition to facilitating SAC response, also functions to mediate silencing of the SAC once the checkpoint has been satisfied. The RZZ complex recruits dynein to the KT, allowing dynein-mediated streaming of SAC proteins from the KT at the onset of anaphase (119). Given FANCC's role in mediating KT recruitment of ZW10, FANCC may play a role not only in SAC activation but also SAC silencing. More work will be needed to explore this possibility.

CDK1 and the FA family

While we have shown that CDK1 phosphorylates FANCC, others have previously demonstrated that FANCG is also phosphorylated by CDK1 during mitosis (120). However, it is not yet known whether CDK1 phosphorylation of FANCG is required for mitotic SAC function of FANCG. It is possible that CDK1 phosphorylation may play an integral role in regulating SAC function of multiple members of the FA pathway. Further studies are needed to explore this possibility.

Significance of serine 543 on FANCC

Our studies have demonstrated that phosphorylation of serine 543 on FANCC is essential not only to its mitotic SAC function, but also to its interphase DNA damage repair function. The mutant S543A demonstrated hypersensitivity to low-dose MMC and a characteristic G2 arrest upon exposure to higher does of MMC. While this demonstrates that addition of the S543A fails to rescue the DNA repair defect of FANCC-deficient fibroblasts, it is unknown whether CDK1 is the kinase responsible for the interphase phosphorylation at this site. The importance of phosphorylation of serine 543 for both interphase and mitotic function of FANCC is intriguing, and suggests that these seemingly separate functions of FANCC may be linked. Likewise, mutation of the CDK1-phosphorylation site in FANCG resulted in MMC hypersensitivity and G2 arrest after MMC treatment (120). In addition to FA proteins, many other SAC proteins have been shown to protect genomic instability not only during mitosis but also via DDR. The SAC protein Bub1 becomes phosphorylated by ATM to participate in DDR (121). Phosphorylation of CHK2, an effector of DDR signaling, by the KT protein hMps1 is necessary for G2/M arrest after DNA damage (122). These proteins play distinct but complementary roles in both SAC and DDR checkpoints to protect genomic integrity. Likewise, we now know not only that FANCC regulates the SAC and DDR, but that its function in both checkpoints is at least in part, dependent on the same phosphorylation site.

Identification of this CDK1 phosphorylation site provides insight into our understanding of how disease may be correlated to patient FANCC mutation status. There are two published records of patients with a mutation at site 543. One of these is an amino acid

substitution S543K “variant of uncertain significance” recorded in ClinVar. The Cancer Genome Atlas (TCGA) has a record of one patient with non-small cell lung cancer (NSCLC) that has a nonsense mutation starting at serine 543 (123). Additionally, many of the mutations in FANCC found in cancers recorded in the TCGA and COSMIC (catalogue of somatic mutations in cancer) databases are located in the C-terminus CDK1-binding region or cause a premature stop codon such that the C-terminus of FANCC is not translated (**Fig. 33**). Given our knowledge that disruption of CDK1-dependent FANCC phosphorylation disrupts both DNA repair and SAC functions of FANCC, we would predict that many of these mutations would have loss of function for the same reason.

Overall, we demonstrate via *in vivo* modeling (**CHAPTER ONE**) that *Fancc* and *Mad2* cooperate to regulate the SAC, and we define a CDK1-FANCC-ZW10 signaling axis (**CHAPTER TWO**) as a mechanism whereby FANCC facilitates SAC function.

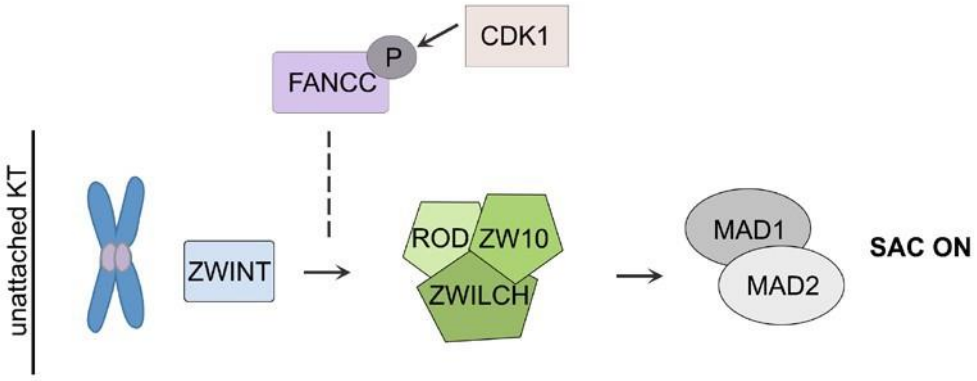

Figure 32. Proposed model for a CDK1-FANCC-ZW10 SAC signaling axis.

Phenotype	Inhibition of Aurora Kinase B	Loss of FANCC
ZWINT KT localization	unaffected	unaffected
ZW10 KT localization	impaired	impaired
SAC disrupted?	yes	yes

Table 3. Phenotypic comparison of the effects of inhibition of Aurora Kinase B and loss of FANCC.

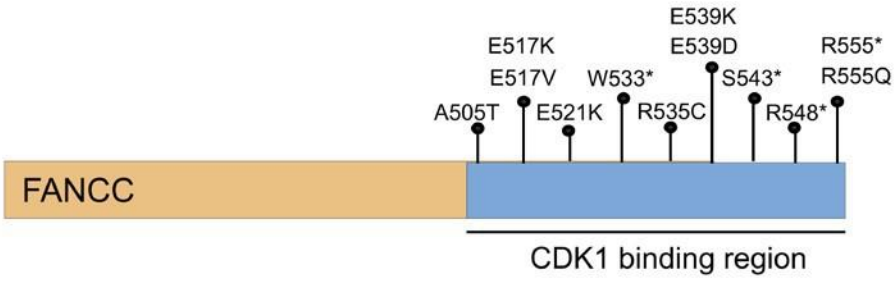

Figure 33. Depiction of amino acid mutations in the CDK1-binding region of FANCC in various cancers. Mutation information was obtained from TCGA and COSMIC databases. Asterisk represents truncating nonsense mutation**.**

FUTURE DIRECTIONS

It is known that the FA family of proteins functions in a complex during interphase to mediate DDR. As we learn more about the role of various FA proteins during mitosis, one main question emerges. Do the FA proteins work in concert or in a complex during mitosis to protect genomic integrity? During mitosis, the FA proteins localize to various mitotic structures. The majority of the FA proteins localize to the centrosome, and FANCA and FANCC are also expressed on the spindle. We also now know that CDK1 phosphorylates FANCC and FANCG. It is possible then that FA proteins act in concert in mitosis to regulate certain mitotic functions, while some FA proteins, such as FANCC, have independent roles during mitosis. We will explore the possibility of a mitotic FA complex by co-immunoprecipitation studies in the future. We will also determine whether loss of certain FA proteins impacts the mitotic localization of other FA proteins using our FA-deficient fibroblasts.

REFERENCES

1. Rosenberg PS, Tamary H, Alter BP. How high are carrier frequencies of rare recessive syndromes? Contemporary estimates for Fanconi Anemia in the United States and Israel. American journal of medical genetics Part A. 2011 Aug;155A(8):1877-83.
2. Auerbach AD. Fanconi anemia and its diagnosis. Mutation research. 2009 Jul 31;668(1-2):4-10.
3. Alter BP, Giri N. Thinking of VACTERL-H? Rule out Fanconi Anemia according to PHENOS. American journal of medical genetics Part A. 2016 Jun;170(6):1520-4.
4. Alter BP, Giri N, Savage SA, Peters JA, Loud JT, Leathwood L, et al. Malignancies and survival patterns in the National Cancer Institute inherited bone marrow failure syndromes cohort study. British journal of haematology. 2010 Jul;150(2):179-88.
5. Auerbach AD. Diagnosis of fanconi anemia by diepoxybutane analysis. Current protocols in human genetics / editorial board, Jonathan L Haines [et al]. 2003 Jul;Chapter 8:Unit 8 7.
6. Shimamura A, Alter BP. Pathophysiology and management of inherited bone marrow failure syndromes. Blood reviews. 2010 May;24(3):101-22.
7. Huck K, Hanenberg H, Gudowius S, Fenk R, Kalb R, Neveling K, et al. Delayed diagnosis and complications of Fanconi anaemia at advanced age--a paradigm. British journal of haematology. 2006 Apr;133(2):188-97.
8. Zhu AX, D'Andrea AD, Sahani DV, Hasserjian RP. Case records of the Massachusetts General Hospital. Case 13-2006. A 50-year-old man with a painful bone mass and lesions in the liver. The New England journal of medicine. 2006 Apr 27;354(17):1828-37.
9. Tolar J, Becker PS, Clapp DW, Hanenberg H, de Heredia CD, Kiem HP, et al. Gene therapy for Fanconi anemia: one step closer to the clinic. Human gene therapy. 2012 Feb;23(2):141-4.
10. Lobitz S, Velleuer E. Guido Fanconi (1892-1979): a jack of all trades. Nature reviews Cancer. 2006 Nov;6(11):893-8.
11. Strathdee CA, Duncan AM, Buchwald M. Evidence for at least four Fanconi anaemia genes including FACC on chromosome 9. Nature genetics. 1992 Jun;1(3):196-8.
12. Strathdee CA, Gavish H, Shannon WR, Buchwald M. Cloning of cDNAs for Fanconi's anaemia by functional complementation. Nature. 1992 Apr 30;356(6372):763-7.
13. Fanconi anaemia/Breast cancer c. Positional cloning of the Fanconi anaemia group A gene. Nature genetics. 1996 Nov;14(3):324-8.
14. Foe JR, Rooimans MA, Bosnoyan-Collins L, Alon N, Wijker M, Parker L, et al. Expression cloning of a cDNA for the major Fanconi anaemia gene, FAA. Nature genetics. 1996 Dec;14(4):488.
15. de Winter JP, Waisfisz Q, Rooimans MA, van Berkel CG, Bosnoyan-Collins L, Alon N, et al. The Fanconi anaemia group G gene FANCG is identical with XRCC9. Nature genetics. 1998 Nov;20(3):281-3.

16. de Winter JP, Leveille F, van Berkel CG, Rooimans MA, van Der Weel L, Steltenpool J, et al. Isolation of a cDNA representing the Fanconi anemia complementation group E gene. American journal of human genetics. 2000 Nov;67(5):1306-8.
17. de Winter JP, Rooimans MA, van Der Weel L, van Berkel CG, Alon N, Bosnoyan-Collins L, et al. The Fanconi anaemia gene FANCF encodes a novel protein with homology to ROM. Nature genetics. 2000 Jan;24(1):15-6.
18. Sawyer SL, Tian L, Kahkonen M, Schwartzentruber J, Kircher M, University of Washington Centre for Mendelian G, et al. Biallelic mutations in BRCA1 cause a new Fanconi anemia subtype. Cancer discovery. 2015 Feb;5(2):135-42.
19. D'Andrea AD. Susceptibility pathways in Fanconi's anemia and breast cancer. The New England journal of medicine. 2010 May 20;362(20):1909-19.
20. Howlett NG, Taniguchi T, Olson S, Cox B, Waisfisz Q, De Die-Smulders C, et al. Biallelic inactivation of BRCA2 in Fanconi anemia. Science. 2002 Jul 26;297(5581):606-9.
21. Hira A, Yoshida K, Sato K, Okuno Y, Shiraishi Y, Chiba K, et al. Mutations in the gene encoding the E2 conjugating enzyme UBE2T cause Fanconi anemia. American journal of human genetics. 2015 Jun 04;96(6):1001-7.
22. Rickman KA, Lach FP, Abhyankar A, Donovan FX, Sanborn EM, Kennedy JA, et al. Deficiency of UBE2T, the E2 Ubiquitin Ligase Necessary for FANCD2 and FANCI Ubiquitination, Causes FA-T Subtype of Fanconi Anemia. Cell reports. 2015 Jul 07;12(1):35-41.
23. Virts EL, Jankowska A, Mackay C, Glaas MF, Wiek C, Kelich SL, et al. AluY-mediated germline deletion, duplication and somatic stem cell reversion in UBE2T defines a new subtype of Fanconi anemia. Human molecular genetics. 2015 Sep 15;24(18):5093-108.
24. Bluteau D, Masliah-Planchon J, Clairmont C, Rousseau A, Ceccaldi R, Dubois d'Enghien C, et al. Biallelic inactivation of REV7 is associated with Fanconi anemia. The Journal of clinical investigation. 2016 Sep 01;126(9):3580-4.
25. Park JY, Virts EL, Jankowska A, Wiek C, Othman M, Chakraborty SC, et al. Complementation of hypersensitivity to DNA interstrand crosslinking agents demonstrates that XRCC2 is a Fanconi anaemia gene. Journal of medical genetics. 2016 Oct;53(10):672-80.
26. Antoniou A, Pharoah PD, Narod S, Risch HA, Eyfjord JE, Hopper JL, et al. Average risks of breast and ovarian cancer associated with BRCA1 or BRCA2 mutations detected in case Series unselected for family history: a combined analysis of 22 studies. American journal of human genetics. 2003 May;72(5):1117-30.
27. Jones S, Hruban RH, Kamiyama M, Borges M, Zhang X, Parsons DW, et al. Exomic sequencing identifies PALB2 as a pancreatic cancer susceptibility gene. Science. 2009 Apr 10;324(5924):217.
28. Antoniou AC, Casadei S, Heikkinen T, Barrowdale D, Pylkas K, Roberts J, et al. Breast-cancer risk in families with mutations in PALB2. The New England journal of medicine. 2014 Aug 7;371(6):497-506.
29. Tischkowitz MD, Morgan NV, Grimwade D, Eddy C, Ball S, Vorechovsky I, et al. Deletion and reduced expression of the Fanconi anemia FANCA gene in sporadic acute myeloid leukemia. Leukemia. 2004 Mar;18(3):420-5.

30. van der Heijden MS, Yeo CJ, Hruban RH, Kern SE. Fanconi anemia gene mutations in young-onset pancreatic cancer. Cancer research. 2003 May 15;63(10):2585-8.
31. Wreesmann VB, Estilo C, Eisele DW, Singh B, Wang SJ. Downregulation of Fanconi anemia genes in sporadic head and neck squamous cell carcinoma. ORL; journal for oto-rhino-laryngology and its related specialties. 2007;69(4):218-25.
32. Ceccaldi R, Sarangi P, D'Andrea AD. The Fanconi anaemia pathway: new players and new functions. Nature reviews Molecular cell biology. 2016 Jun;17(6):337-49.
33. Kottemann MC, Smogorzewska A. Fanconi anaemia and the repair of Watson and Crick DNA crosslinks. Nature. 2013 Jan 17;493(7432):356-63.
34. Du W, Rani R, Sipple J, Schick J, Myers KC, Mehta P, et al. The FA pathway counteracts oxidative stress through selective protection of antioxidant defense gene promoters. Blood. 2012 May 03;119(18):4142-51.
35. Saadatzadeh MR, Bijangi-Vishehsaraei K, Hong P, Bergmann H, Haneline LS. Oxidant hypersensitivity of Fanconi anemia type C-deficient cells is dependent on a redox-regulated apoptotic pathway. The Journal of biological chemistry. 2004 Apr 16;279(16):16805-12.
36. Ridpath JR, Nakamura A, Tano K, Luke AM, Sonoda E, Arakawa H, et al. Cells deficient in the FANC/BRCA pathway are hypersensitive to plasma levels of formaldehyde. Cancer research. 2007 Dec 01;67(23):11117-22.
37. Hira A, Yabe H, Yoshida K, Okuno Y, Shiraishi Y, Chiba K, et al. Variant ALDH2 is associated with accelerated progression of bone marrow failure in Japanese Fanconi anemia patients. Blood. 2013 Oct 31;122(18):3206-9.
38. Sumpter R, Jr., Sirasanagandla S, Fernandez AF, Wei Y, Dong X, Franco L, et al. Fanconi Anemia Proteins Function in Mitophagy and Immunity. Cell. 2016 May 05;165(4):867-81.
39. Pang Q, Keeble W, Christianson TA, Faulkner GR, Bagby GC. FANCC interacts with Hsp70 to protect hematopoietic cells from IFN-gamma/TNF-alpha-mediated cytotoxicity. The EMBO journal. 2001 Aug 15;20(16):4478-89.
40. Haneline LS, Broxmeyer HE, Cooper S, Hangoc G, Carreau M, Buchwald M, et al. Multiple inhibitory cytokines induce deregulated progenitor growth and apoptosis in hematopoietic cells from Fac-/- mice. Blood. 1998 Jun 01;91(11):4092-8.
41. Rathbun RK, Christianson TA, Faulkner GR, Jones G, Keeble W, O'Dwyer M, et al. Interferon-gamma-induced apoptotic responses of Fanconi anemia group C hematopoietic progenitor cells involve caspase 8-dependent activation of caspase 3 family members. Blood. 2000 Dec 15;96(13):4204-11.
42. Dufour C, Corcione A, Svahn J, Haupt R, Poggi V, Beka'ssy AN, et al. TNF-alpha and IFN-gamma are overexpressed in the bone marrow of Fanconi anemia patients and TNF-alpha suppresses erythropoiesis in vitro. Blood. 2003 Sep 15;102(6):2053-9.
43. Nalepa G, Enzor R, Sun Z, Marchal C, Park SJ, Yang Y, et al. Fanconi anemia signaling network regulates the spindle assembly checkpoint. The Journal of clinical investigation. 2013 Sep 3;123(9):3839-47.
44. Abdul-Sater Z, Cerabona D, Potchanant ES, Sun Z, Enzor R, He Y, et al. FANCA safeguards interphase and mitosis during hematopoiesis in vivo. Experimental hematology. 2015 Sep 11.

45. Zou J, Tian F, Li J, Pickner W, Long M, Rezvani K, et al. FancJ regulates interstrand crosslinker induced centrosome amplification through the activation of polo-like kinase 1. Biology open. 2013;2(10):1022-31.
46. Kim S, Hwang SK, Lee M, Kwak H, Son K, Yang J, et al. Fanconi anemia complementation group A (FANCA) localizes to centrosomes and functions in the maintenance of centrosome integrity. The international journal of biochemistry & cell biology. 2013 Sep;45(9):1953-61.
47. Wang HF, Takenaka K, Nakanishi A, Miki Y. BRCA2 and nucleophosmin coregulate centrosome amplification and form a complex with the Rho effector kinase ROCK2. Cancer research. 2011 Jan 01;71(1):68-77.
48. Zou J, Zhang D, Qin G, Chen X, Wang H, Zhang D. BRCA1 and FancJ cooperatively promote interstrand crosslinker induced centrosome amplification through the activation of polo-like kinase 1. Cell cycle. 2014;13(23):3685-97.
49. Ganem NJ, Godinho SA, Pellman D. A mechanism linking extra centrosomes to chromosomal instability. Nature. 2009 Jul 09;460(7252):278-82.
50. Gordon DJ, Resio B, Pellman D. Causes and consequences of aneuploidy in cancer. Nature reviews Genetics. 2012 Mar;13(3):189-203.
51. Chan KL, Palmai-Pallag T, Ying S, Hickson ID. Replication stress induces sister-chromatid bridging at fragile site loci in mitosis. Nature cell biology. 2009 Jun;11(6):753-60.
52. Naim V, Rosselli F. The FANC pathway and BLM collaborate during mitosis to prevent micro-nucleation and chromosome abnormalities. Nature cell biology. 2009 Jun;11(6):761-8.
53. Vinciguerra P, Godinho SA, Parmar K, Pellman D, D'Andrea AD. Cytokinesis failure occurs in Fanconi anemia pathway-deficient murine and human bone marrow hematopoietic cells. The Journal of clinical investigation. 2010 Nov;120(11):3834-42.
54. Ganem NJ, Storchova Z, Pellman D. Tetraploidy, aneuploidy and cancer. Current opinion in genetics & development. 2007 Apr;17(2):157-62.
55. Daniels MJ, Wang Y, Lee M, Venkitaraman AR. Abnormal cytokinesis in cells deficient in the breast cancer susceptibility protein BRCA2. Science. 2004 Oct 29;306(5697):876-9.
56. Takaoka M, Saito H, Takenaka K, Miki Y, Nakanishi A. BRCA2 phosphorylated by PLK1 moves to the midbody to regulate cytokinesis mediated by nonmuscle myosin IIC. Cancer research. 2014 Mar 1;74(5):1518-28.
57. Mondal G, Rowley M, Guidugli L, Wu J, Pankratz VS, Couch FJ. BRCA2 localization to the midbody by filamin A regulates cep55 signaling and completion of cytokinesis. Developmental cell. 2012 Jul 17;23(1):137-52.
58. Boveri T. Concerning the origin of malignant tumours by Theodor Boveri. Translated and annotated by Henry Harris. Journal of cell science. 2008 Jan;121 Suppl 1:1-84.
59. Funk LC, Zasadil LM, Weaver BA. Living in CIN: Mitotic Infidelity and Its Consequences for Tumor Promotion and Suppression. Developmental cell. 2016 Dec 19;39(6):638-52.
60. Parmar K, D'Andrea A, Niedernhofer LJ. Mouse models of Fanconi anemia. Mutation research. 2009 Jul 31;668(1-2):133-40.

61. Vasanthakumar A, Arnovitz S, Marquez R, Lepore J, Rafidi G, Asom A, et al. Brca1 deficiency causes bone marrow failure and spontaneous hematologic malignancies in mice. Blood. 2016 Jan 21;127(3):310-3.
62. Cheng NC, van de Vrugt HJ, van der Valk MA, Oostra AB, Krimpenfort P, de Vries Y, et al. Mice with a targeted disruption of the Fanconi anemia homolog Fanca. Human molecular genetics. 2000 Jul 22;9(12):1805-11.
63. Chen M, Tomkins DJ, Auerbach W, McKerlie C, Youssoufian H, Liu L, et al. Inactivation of Fac in mice produces inducible chromosomal instability and reduced fertility reminiscent of Fanconi anaemia. Nature genetics. 1996 Apr;12(4):448-51.
64. Yang Y, Kuang Y, Montes De Oca R, Hays T, Moreau L, Lu N, et al. Targeted disruption of the murine Fanconi anemia gene, Fancg/Xrcc9. Blood. 2001 Dec 01;98(12):3435-40.
65. Cerabona D, Sun Z, Nalepa G. Leukemia and chromosomal instability in aged Fancc-/- mice. Experimental hematology. 2016 May;44(5):352-7.
66. Pulliam-Leath AC, Ciccone SL, Nalepa G, Li X, Si Y, Miravalle L, et al. Genetic disruption of both Fancc and Fancg in mice recapitulates the hematopoietic manifestations of Fanconi anemia. Blood. 2010 Oct 21;116(16):2915-20.
67. Noll M, Battaile KP, Bateman R, Lax TP, Rathbun K, Reifsteck C, et al. Fanconi anemia group A and C double-mutant mice: functional evidence for a multi-protein Fanconi anemia complex. Experimental hematology. 2002 Jul;30(7):679-88.
68. Carreau M, Gan OI, Liu L, Doedens M, McKerlie C, Dick JE, et al. Bone marrow failure in the Fanconi anemia group C mouse model after DNA damage. Blood. 1998 Apr 15;91(8):2737-44.
69. Freie B, Li X, Ciccone SL, Nawa K, Cooper S, Vogelweid C, et al. Fanconi anemia type C and p53 cooperate in apoptosis and tumorigenesis. Blood. 2003 Dec 01;102(12):4146-52.
70. Houghtaling S, Granville L, Akkari Y, Torimaru Y, Olson S, Finegold M, et al. Heterozygosity for p53 (Trp53+/-) accelerates epithelial tumor formation in fanconi anemia complementation group D2 (Fancd2) knockout mice. Cancer research. 2005 Jan 1;65(1):85-91.
71. Hadjur S, Ung K, Wadsworth L, Dimmick J, Rajcan-Separovic E, Scott RW, et al. Defective hematopoiesis and hepatic steatosis in mice with combined deficiencies of the genes encoding Fancc and Cu/Zn superoxide dismutase. Blood. 2001 Aug 15;98(4):1003-11.
72. Langevin F, Crossan GP, Rosado IV, Arends MJ, Patel KJ. Fancd2 counteracts the toxic effects of naturally produced aldehydes in mice. Nature. 2011 Jul 06;475(7354):53-8.
73. Garaycoechea JI, Crossan GP, Langevin F, Daly M, Arends MJ, Patel KJ. Genotoxic consequences of endogenous aldehydes on mouse haematopoietic stem cell function. Nature. 2012 Sep 27;489(7417):571-5.
74. Zhang QS, Tang W, Deater M, Phan N, Marcogliese AN, Li H, et al. Metformin improves defective hematopoiesis and delays tumor formation in Fanconi anemia mice. Blood. 2016 Dec 15;128(24):2774-84.
75. Ceccaldi R, Parmar K, Mouly E, Delord M, Kim JM, Regairaz M, et al. Bone marrow failure in Fanconi anemia is triggered by an exacerbated p53/p21 DNA damage

response that impairs hematopoietic stem and progenitor cells. Cell stem cell. 2012 Jul 06;11(1):36-49.
76. Zhang H, Kozono DE, O'Connor KW, Vidal-Cardenas S, Rousseau A, Hamilton A, et al. TGF-beta Inhibition Rescues Hematopoietic Stem Cell Defects and Bone Marrow Failure in Fanconi Anemia. Cell stem cell. 2016 May 05;18(5):668-81.
77. Choi E, Park PG, Lee HO, Lee YK, Kang GH, Lee JW, et al. BRCA2 fine-tunes the spindle assembly checkpoint through reinforcement of BubR1 acetylation. Developmental cell. 2012 Feb 14;22(2):295-308.
78. Park I, Lee HO, Choi E, Lee YK, Kwon MS, Min J, et al. Loss of BubR1 acetylation causes defects in spindle assembly checkpoint signaling and promotes tumor formation. The Journal of cell biology. 2013 Jul 22;202(2):295-309.
79. Michel LS, Liberal V, Chatterjee A, Kirchwegger R, Pasche B, Gerald W, et al. MAD2 haplo-insufficiency causes premature anaphase and chromosome instability in mammalian cells. Nature. 2001 Jan 18;409(6818):355-9.
80. Kogan SC, Ward JM, Anver MR, Berman JJ, Brayton C, Cardiff RD, et al. Bethesda proposals for classification of nonlymphoid hematopoietic neoplasms in mice. Blood. 2002 Jul 1;100(1):238-45.
81. Morse HC, 3rd, Anver MR, Fredrickson TN, Haines DC, Harris AW, Harris NL, et al. Bethesda proposals for classification of lymphoid neoplasms in mice. Blood. 2002 Jul 1;100(1):246-58.
82. Dobles M, Liberal V, Scott ML, Benezra R, Sorger PK. Chromosome missegregation and apoptosis in mice lacking the mitotic checkpoint protein Mad2. Cell. 2000 Jun 9;101(6):635-45.
83. Zhang CZ, Spektor A, Cornils H, Francis JM, Jackson EK, Liu S, et al. Chromothripsis from DNA damage in micronuclei. Nature. 2015 Jun 11;522(7555):179-84.
84. Willingale-Theune J, Schweiger M, Hirsch-Kauffmann M, Meek AE, Paulin-Levasseur M, Traub P. Ultrastructure of Fanconi anemia fibroblasts. Journal of cell science. 1989 Aug;93 (Pt 4):651-65.
85. Barton JC, Parmley RT, Carroll AJ, Huang ST, Goodnough LT, Findley HW, Jr., et al. Preleukemia in Fanconi's anemia: hematopoietic cell multinuclearity, membrane duplication, and dysgranulogenesis. Journal of submicroscopic cytology. 1987 Apr;19(2):355-64.
86. Li M, Fang X, Wei Z, York JP, Zhang P. Loss of spindle assembly checkpoint-mediated inhibition of Cdc20 promotes tumorigenesis in mice. The Journal of cell biology. 2009 Jun 15;185(6):983-94.
87. Ricke RM, Jeganathan KB, van Deursen JM. Bub1 overexpression induces aneuploidy and tumor formation through Aurora B kinase hyperactivation. The Journal of cell biology. 2011 Jun 13;193(6):1049-64.
88. Silk AD, Zasadil LM, Holland AJ, Vitre B, Cleveland DW, Weaver BA. Chromosome missegregation rate predicts whether aneuploidy will promote or suppress tumors. Proceedings of the National Academy of Sciences of the United States of America. 2013 Oct 29;110(44):E4134-41.
89. Zasadil LM, Britigan EM, Ryan SD, Kaur C, Guckenberger DJ, Beebe DJ, et al. High rates of chromosome missegregation suppress tumor progression but do not inhibit tumor initiation. Molecular biology of the cell. 2016 Jul 01;27(13):1981-9.

90. Ohashi A, Ohori M, Iwai K, Nakayama Y, Nambu T, Morishita D, et al. Aneuploidy generates proteotoxic stress and DNA damage concurrently with p53-mediated post-mitotic apoptosis in SAC-impaired cells. Nature communications. 2015;6:7668.
91. Ito S, Mantel CR, Han MK, Basu S, Fukuda S, Cooper S, et al. Mad2 is required for optimal hematopoiesis: Mad2 associates with c-Kit in MO7e cells. Blood. 2007 Mar 01;109(5):1923-30.
92. Lordier L, Jalil A, Aurade F, Larbret F, Larghero J, Debili N, et al. Megakaryocyte endomitosis is a failure of late cytokinesis related to defects in the contractile ring and Rho/Rock signaling. Blood. 2008 Oct 15;112(8):3164-74.
93. Wang Q, Liu T, Fang Y, Xie S, Huang X, Mahmood R, et al. BUBR1 deficiency results in abnormal megakaryopoiesis. Blood. 2004 Feb 15;103(4):1278-85.
94. Pawlikowska P, Fouchet P, Vainchenker W, Rosselli F, Naim V. Defective endomitosis during megakaryopoiesis leads to thrombocytopenia in Fanca-/- mice. Blood. 2014 Dec 04;124(24):3613-23.
95. Shi DS, Smith MC, Campbell RA, Zimmerman PW, Franks ZB, Kraemer BF, et al. Proteasome function is required for platelet production. The Journal of clinical investigation. 2014 Sep;124(9):3757-66.
96. Walter D, Lier A, Geiselhart A, Thalheimer FB, Huntscha S, Sobotta MC, et al. Exit from dormancy provokes DNA-damage-induced attrition in haematopoietic stem cells. Nature. 2015 Apr 23;520(7548):549-52.
97. Li X, Le Beau MM, Ciccone S, Yang FC, Freie B, Chen S, et al. Ex vivo culture of Fancc-/- stem/progenitor cells predisposes cells to undergo apoptosis, and surviving stem/progenitor cells display cytogenetic abnormalities and an increased risk of malignancy. Blood. 2005 May 01;105(9):3465-71.
98. Kupfer GM, Yamashita T, Naf D, Suliman A, Asano S, D'Andrea AD. The Fanconi anemia polypeptide, FAC, binds to the cyclin-dependent kinase, cdc2. Blood. 1997 Aug 01;90(3):1047-54.
99. Magron A, Elowe S, Carreau M. The Fanconi Anemia C Protein Binds to and Regulates Stathmin-1 Phosphorylation. PloS one. 2015;10(10):e0140612.
100. Lee SB, Kim JJ, Nam HJ, Gao B, Yin P, Qin B, et al. Parkin Regulates Mitosis and Genomic Stability through Cdc20/Cdh1. Molecular cell. 2015 Oct 01;60(1):21-34.
101. London N, Biggins S. Signalling dynamics in the spindle checkpoint response. Nature reviews Molecular cell biology. 2014 Nov;15(11):736-47.
102. Oliveira RA, Hamilton RS, Pauli A, Davis I, Nasmyth K. Cohesin cleavage and Cdk inhibition trigger formation of daughter nuclei. Nature cell biology. 2010 Feb;12(2):185-92.
103. Skinner JJ, Wood S, Shorter J, Englander SW, Black BE. The Mad2 partial unfolding model: regulating mitosis through Mad2 conformational switching. The Journal of cell biology. 2008 Dec 01;183(5):761-8.
104. Sudakin V, Chan GK, Yen TJ. Checkpoint inhibition of the APC/C in HeLa cells is mediated by a complex of BUBR1, BUB3, CDC20, and MAD2. The Journal of cell biology. 2001 Sep 03;154(5):925-36.
105. Shepperd LA, Meadows JC, Sochaj AM, Lancaster TC, Zou J, Buttrick GJ, et al. Phosphodependent recruitment of Bub1 and Bub3 to Spc7/KNL1 by Mph1 kinase maintains the spindle checkpoint. Current biology : CB. 2012 May 22;22(10):891-9.

106. Buffin E, Lefebvre C, Huang J, Gagou ME, Karess RE. Recruitment of Mad2 to the kinetochore requires the Rod/Zw10 complex. Current biology : CB. 2005 May 10;15(9):856-61.
107. Kops GJ, Kim Y, Weaver BA, Mao Y, McLeod I, Yates JR, 3rd, et al. ZW10 links mitotic checkpoint signaling to the structural kinetochore. The Journal of cell biology. 2005 Apr 11;169(1):49-60.
108. Silio V, McAinsh AD, Millar JB. KNL1-Bubs and RZZ Provide Two Separable Pathways for Checkpoint Activation at Human Kinetochores. Developmental cell. 2015 Dec 07;35(5):600-13.
109. Collin P, Nashchekina O, Walker R, Pines J. The spindle assembly checkpoint works like a rheostat rather than a toggle switch. Nature cell biology. 2013 Nov;15(11):1378-85.
110. Famulski JK, Vos L, Sun X, Chan G. Stable hZW10 kinetochore residency, mediated by hZwint-1 interaction, is essential for the mitotic checkpoint. The Journal of cell biology. 2008 Feb 11;180(3):507-20.
111. Kasuboski JM, Bader JR, Vaughan PS, Tauhata SB, Winding M, Morrissey MA, et al. Zwint-1 is a novel Aurora B substrate required for the assembly of a dynein-binding platform on kinetochores. Molecular biology of the cell. 2011 Sep;22(18):3318-30.
112. Reuter TY, Medhurst AL, Waisfisz Q, Zhi Y, Herterich S, Hoehn H, et al. Yeast two-hybrid screens imply involvement of Fanconi anemia proteins in transcription regulation, cell signaling, oxidative metabolism, and cellular transport. Experimental cell research. 2003 Oct 01;289(2):211-21.
113. Funabiki H, Wynne DJ. Making an effective switch at the kinetochore by phosphorylation and dephosphorylation. Chromosoma. 2013 Jun;122(3):135-58.
114. Voets E, Marsman J, Demmers J, Beijersbergen R, Wolthuis R. The lethal response to Cdk1 inhibition depends on sister chromatid alignment errors generated by KIF4 and isoform 1 of PRC1. Scientific reports. 2015 Oct 01;5:14798.
115. Blom N, Gammeltoft S, Brunak S. Sequence and structure-based prediction of eukaryotic protein phosphorylation sites. Journal of molecular biology. 1999 Dec 17;294(5):1351-62.
116. Blom N, Sicheritz-Ponten T, Gupta R, Gammeltoft S, Brunak S. Prediction of post-translational glycosylation and phosphorylation of proteins from the amino acid sequence. Proteomics. 2004 Jun;4(6):1633-49.
117. Huang F, Ben Aissa M, Magron A, Huard CC, Godin C, Levesque G, et al. The Fanconi anemia group C protein interacts with uncoordinated 5A and delays apoptosis. PloS one. 2014;9(3):e92811.
118. Scaerou F, Starr DA, Piano F, Papoulas O, Karess RE, Goldberg ML. The ZW10 and Rough Deal checkpoint proteins function together in a large, evolutionarily conserved complex targeted to the kinetochore. Journal of cell science. 2001 Sep;114(Pt 17):3103-14.
119. Howell BJ, McEwen BF, Canman JC, Hoffman DB, Farrar EM, Rieder CL, et al. Cytoplasmic dynein/dynactin drives kinetochore protein transport to the spindle poles and has a role in mitotic spindle checkpoint inactivation. The Journal of cell biology. 2001 Dec 24;155(7):1159-72.

120. Mi J, Qiao F, Wilson JB, High AA, Schroeder MJ, Stukenberg PT, et al. FANCG is phosphorylated at serines 383 and 387 during mitosis. Molecular and cellular biology. 2004 Oct;24(19):8576-85.
121. Yang C, Wang H, Xu Y, Brinkman KL, Ishiyama H, Wong ST, et al. The kinetochore protein Bub1 participates in the DNA damage response. DNA repair. 2012 Feb 01;11(2):185-91.
122. Wei JH, Chou YF, Ou YH, Yeh YH, Tyan SW, Sun TP, et al. TTK/hMps1 participates in the regulation of DNA damage checkpoint response by phosphorylating CHK2 on threonine 68. The Journal of biological chemistry. 2005 Mar 04;280(9):7748-57.
123. Campbell JD, Alexandrov A, Kim J, Wala J, Berger AH, Pedamallu CS, et al. Distinct patterns of somatic genome alterations in lung adenocarcinomas and squamous cell carcinomas. Nature genetics. 2016 Jun;48(6):607-16.

CURRICULUM VITAE

Donna Marie Edwards

EDUCATION

2011-present: Medical Scientist Training Program, Indiana University; Indianapolis, IN.

M.D. training, Indiana University School of Medicine

2011-2013 (First two years of medical school) Earned "Honors" grade in following medical school courses: Biochemistry, Cellular and Molecular Biology, Histology, Physiology, Immunology, Microbiology, General Pathology, Systemic Pathology, Neuroscience, Pharmacology, and Introduction to Clinical Medicine.

Present-2019 3rd and 4th years of medical school.

Ph.D., Department of Biochemistry and Molecular Biology

2013-2017: PhD student in laboratories of Dr. Clapp and Dr. Nalepa. PhD conferred in June 2017 from Indiana University.

2007-2011: University of Notre Dame, Notre Dame, IN.

B.S. in Biology
Graduated *summa cum laude*, GPA: 3.96

ACADEMIC AND PROFESSIONAL HONORS

2016 Merilyn Hester Scholarship, Indiana University Simon Cancer Center

2015 Indiana University School of Medicine Graduate Student Travel Award

2015 American Society of Hematology Abstract Achievement Award

2015 International Society of Experimental Hematology Annual Scientific Meeting Travel Grant Award

2015 Indiana University Purdue University Indianapolis (IUPUI) Elite 50 graduate student award

2014 Biochemistry Research Day Poster Award, Indiana University Department of Biochemistry & Molecular Biology

2014 Dean's Office Medical School Travel Grant Award

2014 American Society of Hematology Abstract Achievement Award

2014 Indiana Clinical Translational Sciences Initiative (CTSI) Predoctoral Award

2011 Summa Cum Laude; University of Notre Dame, Notre Dame, IN

RESEARCH EXPERIENCE

2013-2017 Graduate student, Laboratory of Dr. Grzegorz Nalepa & Dr. Wade Clapp. Indiana University School of Medicine, Indianapolis, IN.

2009-2011 Undergraduate Research Assistant, Laboratory of Dr. Robert Schulz. University of Notre Dame, Notre Dame, IN.

2010 Undergraduate Research Assistant, Prospective Physician-Scientists Research Program, Laboratory of Dr. Wade Clapp. Indiana University School of Medicine, Indianapolis, IN.

2009 Undergraduate Research Assistant, NSF Summer Research Experience for Undergraduates, Laboratory of Dr. Robert Schulz. University of Notre Dame, Notre Dame, IN

CLINICAL EXPERIENCE

2011-present Medical Student, Indiana University School of Medicine, Indianapolis, IN.

2011-present Student Outreach Clinic Volunteer, Indiana University School of Medicine, Indianapolis, IN.

2005-2008 Northwest Community Hospital Volunteer, Arlington Heights, IL.

POSITIONS AND EMPLOYMENT

2012-2015 Creative Arts Therapy Student Interest Group, Director of Members, Indiana University School of Medicine, Indianapolis, IN.

2010-2011 Resident Assistant, Office of Residence Life & Housing, University of Notre Dame, Notre Dame, IN.

2007-2011 Administrative Assistant, Alumni Association, University of Notre Dame, Notre Dame, IN.

2008-2010 Introductory Biology Lab Teaching Assistant, University of Notre Dame, IN.

2008 Care Package Retail Representative, Northwest Community Hospital Marketing Department, Arlington Heights, IL.

2007-2008 Sales Associate, Macy's Department Store, Schaumburg, IL.

PROFESSIONAL SOCIETIES

2015-present International Society of Experimental Hematology, Student Member.

2013-present American Society of Hematology, Medical Student Member.

2011 Phi Beta Kappa Honor Society Member, Notre Dame Chapter, IN.

2011 National Collegiate Hispanic Honor Society Member, Sigma Delta Pi, Notre Dame Chapter, IN.

TRAINING GRANTS AND FELLOWSHIPS

2016-2018 NCI Ruth L. Kirschstein National Research Service F30 Individual Fellowship Award Grant#1F30CA200227.

2015-2016 NIH T32 HL007910 Predoctoral Fellowship Award "Basic Science Studies on Gene Therapy of Blood Diseases" (PI: Broxymeyer).

2014-2015 Indiana Clinical and Translational Sciences Institute (CTSI) Predoctoral Award-Grant#UL1TR001108 (A. Shekhar, PI.)

2011-present Medical Scientist Training Program Fellow, Indiana University School of Medicine, Indianapolis, IN

ABSTRACTS AND POSTERS

1. *Cdkn3 Knockout Mice Develop Hematopoietic Malignancies.* Zejin Sun, **Donna Cerabona***, Ying He, Grzegorz Nalepa. American Society of Hematology National Conference, San Diego, CA (December 2016). *presenting author.

2. *Impaired Spindle Assembly Checkpoint In Vivo Promotes MDS/AML in a Novel Mouse Model of Fanconi Anemia.* **Donna Cerabona**, Zahi Abdul Sater, Elizabeth Sierra Potchanant, Ying He, Zejin Sun, Grzegorz Nalepa. American Society of Hematology National Conference, Orlando FL (December 2015).

3. *Fanconi anemia pathway safeguards interphase and mitosis in vivo*. **Donna Cerabona.** Zahi Abdul-Sater, Elizabeth Sierra Potchanant, Zejin Sun, Rikki Enzor, Ying He, Kent Robertson, Scott Goebel, Grzegorz Nalepa. International Society for Experimental Hematology annual conference, Kyoto, Japan (September 2015).

4. *The Fanoni anemia (FA) signaling network regulates the spindle assembly checkpoint to prevent aneuploidy and cancer in vivo: lessons from a new murine model of FA.* **Donna Cerabona**, Wade Clapp, and Grzegorz Nalepa. Indiana Clinical & Translational Sciences Institute (CTSI) annual conference, Indianapolis, IN (September 2014).

5. *The Fanoni anemia (FA) signaling network regulates the spindle assembly checkpoint to prevent aneuploidy and cancer in vivo: lessons from a new murine model of FA.* **Donna Cerabona**, Wade Clapp, and Grzegorz Nalepa. National M.D./Ph.D. Student Conference, Keystone, Colorado (July 2014).

6. *FANCA controls mitotic phosphosignaling networks to ensure genome stability during cell division.* Rikki Enzor, Zahi Abdul Sater, **Donna Cerabona**, Zejin Sun, Su-Jung Park, Helmut Hanenberg, D. Wade Clapp and Grzegorz Nalepa. American Society of Hematology National Conference, New Orleans, LA (December 2013).

7. *The PI3K catalytic subunit p110 delta is a crucial mediator of leukemia-associated mutant PTPN11-induced GM-CSF hypersensitivity*. Charles B Goodwin, Rachel L. Gearinger, Raghuveer Mali, **Donna Cerabona**, Gordon Chan, Benjamin G. Neel, Reuben Kapur, Rebecca J. Chan. European Working Group of MDS/JMML Meeting, Prague (2012).

8. *TGFβ-Mediated Alteration of Sphingolipid Metabolism as a Potential Determinant in Osteolytic Bone Metastasis.* Keith R. Stayrook, Yong Wei, **Donna Cerabona**, Maryla Niewolna, Pierrick G. Fournier, Daniel F. Edwards, Khalid S. Mohammad, Yibin Kang, and Theresa A. Guise. ASBMR/IU Cancer Research Day, Indianapolis, IN (2012).

9. *Analysis of M2(H37A) Cytotoxic Activity as a Tool for Drosophila Cell Ablation Technology*. **Donna M. Cerabona**, Victoria K. Lam, and Robert A. Schulz. Science and Engineering Undergraduate Symposium, University of Notre Dame, (July 2009).

ORAL PRESENTATIONS

1. *Genomic Instability in Fanconi anemia results from a combination of chromosome mis-segregation in mitosis and unresolved interphase DNA damage.* **Donna Cerabona**, Zahi Abdul Sater, Grzegorz Nalepa. American Society of Hematology National meeting, San Francisco, CA (December 2014).

PEER-REVIEWED PUBLICATIONS

1. INPP5E preserves genomic stability through regulation of mitosis. Sierra Potchanant EA, **Cerabona D**, Sater ZA, He Y, Sun Z, Gehlhausen J, Nalepa, G. Mol. Cell Biol. 2017 Mar 1;37(6).

2. Leukemia and chromosomal instability in aged Fancc-/- mice. **Cerabona D**, Sun Z, Nalepa G. Exp Hematol. 2016 May;44(5):352-7.

3. FANCA safeguards interphase and mitosis during hematopoiesis in vivo. Abdul-Sater Z*, **Cerabona D*.** Potchanant ES, Sun Z, Enzor R, He Y, Robertson K, Goebel WS, Nalepa G. Exp Hematol. 2015 Dec;43(12):1031-1046. *authors contributed equally to work.

4. TGF**β**-mediated induction of SphK1 as a potential determinant in osteolytic bone metastasis. Stayrook KR, Mack JK, **Cerabona D**, Edwards DF, Bui HH, Niewolna M, Fournier PGJ, Mohammad KS, Waning DA, Guise TA. BoneKey Rep. 2015 Jul 8;4:719.

5. Normal hematopoiesis and neurofibromin-deficient myeloproliferative disease require Erk. Staser K, Park SJ, Rhodes SD, Zeng Y, He YZ, Shew MA, Gehlhausen JR, **Cerabona D**, Menon K, Chen S, Sun Z, Yuan J, Ingram DA, Nalepa G, Yang FC, Clapp DW. J Clin Invest. 2013 Jan 2;123(1):329-34.

6. Specific cell ablation in *Drosophila* using the toxic viral protein M2(H37A). Lam VK, Tokusumi T, **Cerabona D,** Schulz RA. Fly 2010 Oct-Dec;4(4):338-343.

.